CR—208603

IN-42
31495

Semi-Annual Report on

Coupling Processes

between

Atmospheric Chemistry and Climate

NAS5-97039

by

M. K. W. Ko, Debra Weisenstein, Run-Lie Shia, and N. D. Sze

Atmospheric and Environmental Research, Inc.

840 Memorial Drive

Cambridge, MA 02139

Prepared for

NASA Atmospheric Chemistry Modeling and Data Analysis Program

September 18, 1998

Table of Content

(I)	**Model Simulation of the future behavior of ozone through 2050, results for Chapter 12 of *WMO Ozone Assessment Report***	**2**
(II)	**Atmospheric lifetimes of source gases, contribution to Chapter 1 of *WMO Ozone Assessment Report***	**3**
(III)	**Contributions to the preparation of the 1998 *WMO Ozone Assessment Report***	**6**
(IV)	**Model and Measurement Workshop Report**	**7**
(V)	**The POLARIS Campaign**	**8**
(VI)	**Publications supported by this contract**	**9**
(VII)	**References Cited**	**15**

Appendix A: Calculations of Ozone Trends in the AER 2-D Model: Sensitivity to Interannual Temperature Variations and Transport Barriers

Appendix B: Models & Measurements II Workshop Report Source Gas

Appendix C: Results of the Model & Measurement Workshop II: Implications for Future AESA Assessments

Atmospheric and Environmental Research, Inc.

840 Memorial Drive
Cambridge, Massachusetts
02139-3771

Telephone
617 547-6207

Facsimile
617 661-6479

www.aer.com

18 September, 1998

Cynthia Dean
Contracting Officer
National Aeronautics and Space Administration
Mail Code: 219
Goddard Space Flight Center
Earth Sciences Procurement Office
Greenbelt, MD 20771

re: Contract NAS5-97039

Dear Cynthia,

Enclosed please find the Semi-Annual Report on Coupling Processes between Atmospheric Chemistry and Climate.

Please get in touch with me if you have any questions.

Yours Sincerely,

Malcolm Ko

Encl:

Cc: Center for Aerospace Information (2)
Richard Stewart, Contracting Officer's Technical Representative (5)
Publications and Graphics Services Section (1)
Cecilia Sze, AER (P698)

Abstract

This is the third semi-annual report for NAS5-97039, covering the time period January through June 1998. The overall objective of this project is to improve the understanding of coupling processes between atmospheric chemistry and climate. Model predictions of the future distributions of trace gases in the atmosphere constitute an important component of the input necessary for quantitative assessments of global change. We will concentrate on the changes in ozone and stratospheric sulfate aerosol, with emphasis on how ozone in the lower stratosphere would respond to natural or anthropogenic changes.

The key modeling tools for this work are the AER two-dimensional chemistry-transport model, the AER two-dimensional stratospheric sulfate model, and the AER three-wave interactive model with full chemistry. We will continue developing our three-wave model so that we can help NASA determine the strengths and weakness of the next generation assessment models.

(I) Model simulation of the future behavior of ozone through 2050, results for Chapter 12 of *WMO Ozone Assessment Report*

AER provided 2-D model calculations of past and future ozone trends for Chapter 12 of the WMO/UNEP 1998 Ozone Assessment. Chapter 12 is entitled "Predicting Future Ozone Changes and Detection of Recovery" with lead authors John Pyle and David Hofmann. Section 12.2 deals with calculated ozone changes and was authored by Doug Kinnison. AER provided calculated results for Scenario A from 1979-1995 and Scenario A3 from 1996-2050. Figure 12.9 of the draft report shows these results and is reproduced here as Figure 1. These calculations used year-by-year temperatures from NCEP. A plot of the AER calculated ozone trends from 1979 to 1995 using both climatological and year-by-year temperatures appears as Figure 12.7 in the draft report and as Figure 2 here.

At the Spring 1998 AGU meeting in Boston, Debra Weisenstein presented a poster entitled "Calculations of ozone trends in the AER 2-D model: Sensitivity to interannual temperature variations and transport barriers". The study presented included the ozone trend calculations from 1979 to 1995 generated for WMO and additional sensitivity studies for the same time period. To study sensitivity to input temperature and aerosol surface area, the calculation was performed with (A) only trace gas increases; (B) with trace gas increases and aerosol surface area variations; (C) with trace gas increases, aerosol surface area variations, and zonal mean temperature variations; and (D) with trace gas increases, aerosol surface area variations, and variations in both the zonal mean and distribution of temperature. Figure 3 shows the calculated change in annual average column ozone from 1979-1995 for the 4 scenarios just mentioned. It can be seen that use of year-by-year temperatures in the model adds year-by-year changes to the calculated ozone trends, though disagreements with TOMS data remain. The lack of year-by-year variations in transport is one possible explanation.

Transport sensitivities were approached by repeating the 1979-1995 trend calculations with 2 alternate circulations. The first, designated the "AER Slow Circulation", was derived by scaling the advective winds in the standard AER model by 0.6 to slow down the transport. The second transport circulation employed both the advective winds and eddy diffusion coefficients of the GSFC 2-D model. Both these alternate circulations produce total ozone maps for 1990 which resemble the TOMS data more closely than the standard AER model. Calculated ozone trends with these circulations are shown in Figure 4. The two AER circulations produce very similar ozone trends. The GSFC circulation yields excessive ozone depletion in 1993, a result of excess depletion in the southern hemisphere for that year.

A copy of the presentation made at the AGU meeting is included as Appendix A.

(II) Atmospheric lifetimes of source gases, contribution to Chapter 1 of *WMO Ozone Assessment Report*

The WMO Assessment report (WMO, 1995) gave a set of reference steady-state lifetimes for use in calculations of ozone depletion potentials and global warming potentials. The same reference lifetimes were also used as response times in halogen loading calculations. With the exception of CFC-11, the WMO (1995) reference lifetimes for the species listed are the mean values of model results from several groups reported in Kaye *et al.* (1994). Because CFC-11 is used as the reference gas in the definition of the ozone depletion potential, extra care was used in selecting its WMO (1995) reference value, basing it on observations as well as model calculations.

Table II.1 lists the model calculated steady state lifetimes. Several 2-D models have modified their transport parameters to simulate the effect of a tropical barrier. Results from the AER model show that restricting the mixing through the barrier leads to shorter calculated lifetimes (Shia *et al.*, 1998). A second observation is that the lifetimes for CFC-11 and CCl_4 from two of the three 3-D models are much shorter than those calculated by the 2-D models. It could be argued that lifetimes calculated by 3-D models may be more realistic since they have a more direct (*i.e.*, 3-D) representation of the transport processes in the atmosphere. However, more work is needed to assure that the vertical resolution in such models is sufficient to resolve the scale heights of the species with short local lifetimes.

The Volk *et al.* (1997) formalism provides, for the first time, a way to obtain steady-state stratospheric lifetimes from observations. With the exception of Halon-1211, the species listed in Table II.2 have very little removal in the troposphere. As a result, the derived stratospheric lifetimes can be compared directly to atmospheric lifetimes. As is evident in Table II.2, the derived lifetimes for CFC-11, CCl_4, and CFC-12 are in the shorter end of the model range, and shorter than the WMO (1995) reference lifetimes (see Table II.3). It is also interesting to note that the derived shorter lifetimes are in better agreement with the lifetimes calculated by two of the three 3-D models in Table II.1. The large uncertainties in the derived lifetimes given in column 3 of Table II.2 arise from the uncertainty in the SF_6 measurement made during the 1994 ASHOE/MAESA campaign. The uncertainty has been reduced in subsequent flights. The lifetimes relative to CFC-11 derived by Volk *et al.* (1997) have much smaller uncertainties because $d\sigma_i/d\sigma_{CFC\text{-}11}$ can be determined more accurately. When referenced to a CFC-11 lifetime of either 45 years (Table II.3, column 6) or 50 years (Table II.3, column 5), with the exception of CCl_4 and Halon-1211, these derived lifetimes agree within their uncertainties and with the WMO (1995) reference lifetimes.

Butler *et al.* (1998) showed that the observed burden of Halon-1211 is inconsistent with the emissions if one uses the reference lifetime of 20 years. The WMO (1995) reference lifetime of 20 years was obtained by averaging the model results from Kaye *et al.* (1994). Because of disagreement between the measurements of Gillotay and Simon (1989) and Burkholder *et al.* (1991) for the absorption cross sections for wavelengths longer than 288 nm, the JPL Data Evaluation Panel did not give any recommended values for these wavelengths (DeMore *et al.*, 1997). Burkholder *et al.* (1991) estimated the partial lifetime due to photolysis in the long-wavelength region to be about 20 years. Combining this with the estimated stratospheric lifetime of 20 years from Volk et al. (1997) would give an atmospheric lifetime of about 10 years. Table II.1 shows calculated lifetimes from several models with different cross-sections. It is likely that some models ignored the long wave photolysis in their calculations and biased the average towards longer lifetimes.

The WMO (1995) value of 50 years for CFC-11 is in good agreement with the central estimate of the lifetime from ALE/GAGE/AGAGE measurements (Cunnold *et al.*, 1997), but not with the central estimate of 41 years by Volk *et al.* (1997). The derived lifetime range for CFC-11 using the Volk *et al.* (1997) method (29 to 53 years) just includes the value of 50 years. However, a new reference value between 41 and 50 years would lie well within the ranges of both the Cunnold *et al.* (1997) and Volk *et al.* (1997) estimates.

Given this information, it would be appropriate to reevaluate the recommended lifetimes of some of these gases.

Table II-1. Model-calculated steady-state lifetimes in years.

SPECIES	AER[a]	GSFC[a]	CSIRO[a]	Harvard 2-D[a]	LLNL[a]	SUNY -SPB[a]	UNIVAQ 2-D[a]	LaRC 3-D[a]	GISS-UCI 3-D[b]	MIT 3-D[c]
N_2O	109	130	117	122	106	125	122	175	113	124
CCl_3F	47	61	53	68	49	49	44	57	35	42
CCl_2F_2	92	111	100	106	92	107	105	149	90	107
$C_2Cl_3F_3$	77	101	83	55	81	87	81	-	70	79
CCl_4	41	53	46	64	42	39	36	42	28	30
$CBrClF_2$ (H-1211)	16[d]	12[e]	36[f]	-	-	-	21[f]	29[f]	21	-
$CBrF_3$ (H-1301)	63	78	69	-	-	-	61	93	52	-

[a] Results are taken from the Model and Measurement Workshop II (M&M I). The models and the contact persons are as follows: AER - Atmospheric and Environmental Research, Inc., USA, Malcolm Ko; GSFC - NASA Goddard Space Flight Center, USA, Charles Jackman; CSIRO - Commonwealth Scientific and Industrial Research Organisation (CSIRO)

Telecommunications and Industrial Physics, Australia, Keith Ryan; Harvard 2-D - Harvard University, Hans Schneider; LLNL - Lawrence Livermore National Laboratory, USA, Doug Kinnison; SUNY-SPB - State University of New York at Stony Brook, Marvin Geller; UNIVAQ 2-D - University of l'Aquila, Italy, Giovanni Pitari; LaRC 3-D - NASA Langley Research Center, USA, William Grose. LaRC is the only 3-D model that participated in M&M II.

[b] Results given are for steady-state lifetimes from Avallone and Prather (1997). The values should be close to the atmospheric lifetimes except for Halon-1211.

[c] Results for MIT model from Table 5-2 of Kaye *et al.* (1994). MIT model described in Golombek and Prinn (1993) and references therein.

[d] Calculated using cross section from Burkholder *et al.* (1991).

[e] Calculated using cross section from DeMore *et al.* (1987).

[f] Calculated using the Halon-1211 cross section from DeMore *et al.* (1997) that did not give any recommendation beyond 288 nm.

Table II.2. Stratospheric steady-state lifetimes (from Volk *et al.*, 1997).

Species	Observed $d\chi_i/d\Gamma$ from ASHOE/MAESA (ppt yr^{-1}, ±%)	Steady-state lifetime based on corrected gradient with respect to age (years ± years)	$d\chi_i/d\chi_{CFC\text{-}11}$ observed correlation slope relative to CFC-11 from ASHOE/MAESA (ppt/ppt, ± %)	Steady-state lifetime based on corrected correlation slope and $\tau_{CFC\text{-}11} = 45 \pm 7$ years (years ± years)	Correction factor for tropospheric growth $C(\chi_i)$
N_2O	-13,000 ± 38%	124 ± 49	436 ± 11%	122 ± 22	0.97 ± 0.02
CCl_3F	-33.5 ± 28%	41 ± 12		(45 ± 7)	0.96 ± 0.02
CCl_2F_2	-43.8 ± 25%	77 ± 26	1.29 ± 7%	87 ± 17	0.77 ± 0.07
CCl_2FCClF_2	-7.3 ± 22%	89 ± 35	0.212 ± 20%	100 ± 32	0.65 ± 0.12
CCl_4	-15.9 ± 32%	32 ± 11	0.515 ± 3.6%	32 ± 6	1.03 ± 0.02
$CBrClF_2$ (H-1211)	-0.84 ± 31%	20 ± 9	0.0237 ± 7%	24 ± 6	0.90 ± 0.10

Table II.3. Comparison of reference steady-state lifetimes from WMO [1995] with model-calculated ranges and lifetimes derived from observations. All lifetimes are in years.

	Reference Lifetimes from WMO [1995] [a]	Model Range [b]	Volk SF_6 [c]	Volk CFC-11 [d] (50 Year)	Volk CFC-11 [d] (45 Year)	Minschwaner UARS [g]	AGAGE [e]
N_2O	120	106-175	124 ± 49	135 ± 16	122 ± 22	117 ± 26	
CCl_3F	50	35-68	41 ± 12	50[d]	(45 ± 7)		52 (40-76)
CCl_2F_2	102	90-149	77 ± 26	96 ± 12	87 ± 17	103 ± 25	185 (105-770)
$C_2Cl_3F_3$	85	55-101	89 ± 35	112 ± 31	100 ± 32		
CCl_4	42	28-64	32 ± 11	36 ± 4	32 ± 6		
$CBrClF_2$ (H-1211)	20	12-36	20 ± 9[f]	26 ± 5[f]	24 ± 6		
$CBrF_3$ (H-1301)	65	61-93					

[a] From Table 13-1, WMO (1995)

[b] From Table 1-4

[c] Derived steady-state stratospheric lifetimes based on gradient with age derived from SF_6 data, from Volk *et al.* (1997).

[d] Derived steady-state stratospheric lifetimes based on gradient with CFC-11 and an adopted lifetime of 50 years for CFC-11, from WMO (1995). Compare to values based on 45 years from Table 1-5.

[e] From Table 1-6. The range is calculated using the uncertainty in the inverse lifetime given in the table.

[f] Since Halon-1211 is dissociated by photolysis in the longwave, there is significant removal in the troposphere so that the stratospheric lifetimes should not be compared directly to the global lifetime. See text for further discussion.

[g] Steady-state lifetime from Minschwaner *et al.* (1998) derived using UARS observations, assumed mean age, and tropospheric growth rates.

(III) Contributions to the preparation of the 1998 *WMO Ozone Assessment Report*

Malcolm Ko is a co-author for Chapter 1, "Long-lived Ozone-Related Compounds", of the *WMO Ozone Assessment Report.* The lead authors are Ronald Prinn and Rudolf Zander.

Malcolm Ko worked with Michael Volk to prepare a section on the atmospheric lifetimes of the long-lived gases as can be determined from model calculations and observations. The model calculated lifetimes are taken from the Models and Measurements Workshop (II) calculations. The results from observations are taken from Volk et al. (1997) which uses historical records of tropospheric measurement to correct the observed correlation in the lower stratosphere to obtain steady state lifetimes. One result of the study is that there are indications that the lifetime of CFC-11 may be shorter than the currently accepted value of 50 years. A clearer picture should emerge when the uncertainty in the lifetime can be reduced. One conclusion of the Chapter is that the reference lifetime of CFC-11 should be evaluated given the new information available since the Kaye et al. Lifetime report (see section I).

Malcolm Ko attended the Chapter co-authors meeting in January 1998 at Boulder Colorado, and worked with the lead authors to revise the chapter after the Review meeting in June, 1998.

Jose Rodriguez is lead author for Chapter 2 along with Michael Kurylo. Jose's effort is funded by this project. Chapter 2, entitled "Short-lived Ozone-related Compounds", deals with source gases that are removed by OH in the troposphere. A large part of the chapter was devoted to methyl bromine (CH_3Br), including its ozone depletion potential. Jose attended the co-authors meeting for Chapter 2 in January 1998 at Boulder Colorado. He also attended the Review meeting held in Les Diablet, Switzerland in June, 1998.

We also performed some chlorine loading calculations and communicated our results to Guus Velder who is one of the lead authors of Chapter 11. Finally, results from a 1970-2050 trend calculation with the AER 2-D CTM were submitted to Chapter 12 by the January 1998 deadline (see section I of this report).

(IV) Model and Measurement Workshop Report

Our contributions to the Model and Measurement workshop consist of participation in the definition of the numerical experiments, providing results from the AER 2-D model, and writing the section on comparison of model simulated and observed concentrations of the source gases. A copy of the section is included in Appendix B.

Malcolm Ko attended the Model and Measurement Workshop meeting in March 1998 at Satellite Beach, Florida. The consensus of the people present was that the report should adopt the following philosophy:

(1) New observations have provided us numerous case studies to test our current understanding of chemistry controlling the partitioning of the radicals. This is an important step in determining the local production and removal rate of ozone and others trace gases. Calculations using the photochemical steady-state (PSS) model confirmed that the current adopted photochemistry data, by and large, are adequate. In addition, Ross Salawitch can use the same PSS to verify the partitioning calculated in each of the participating models.

(2) New observations of trace gases, SF_6 and CO_2, in particular, provide new constraints on the transport rates in the atmosphere. Many of these can be translated to scaler quantities that could be compared to values obtained from various numerical experiments that were performed.

(3) Comparison of the model calculated NO_y, Cl_y and O_3 with observations provides indications of whether the photochemistry test and transport diagnostics provide useful criteria to assign confidence levels for the model results. The perturbation runs will also allow us to determine if the model calculated ozone response could likewise be separated according to those same criteria.

Malcolm Ko made a presentation at the High Speed Research Program meeting at Virginia Beach, April 1998 summarizing point (3). A copy of the presentation material is included in appendix C.

The participants also agreed on a tentative publication schedule. Malcolm Ko, Charles Jackman, Alan Plumb and Jae Park will work on the executive summary and final editing of the report.

(V) The POLARIS Campaign

Malcolm Ko and Hope Michelsen attended the POLARIS science team meeting at Snowmass Village, Colorado, June 1998. The participants agreed on a schedule to submit a group of papers to the *Journal Geophysical Research*. Courtney Scott will be first author on a paper discussing the sensitivity of model calculated age of air to changes in transport parameters in a 2-D chemistry-transport model. We will also participate in one other paper by Osterman et al. "The budget and partitioning of reactive nitrogen species in the Arctic stratosphere".

(VI) Publications supported by this contract

Papers that have appeared or are in press

(1) Ko, M.K.W., N-D. Sze, C. Scott, and D.K. Weisenstein, (1997), On the relation between stratospheric chlorine/bromine loading and short-lived tropospheric source gases, submitted to *J. Geophys. Res.* **102**, D21, 25507-25517.

Current methods for estimating the concentrations of inorganic chlorine/bromine species (Cl_y/Br_y) in the stratosphere due to decomposition of tropospheric source gases assume that the Cl_y/Br_y concentration in the stratosphere is determined mainly by the balance between production from in situ oxidation of the source gases in the stratosphere and removal by transport of Cl_y/Br_y out of the stratosphere. The rationale being that, for source gases whose lifetime is of order several months or longer, the concentration of Cl_y/Br_y in the troposphere is small because they are produced at a relatively slow rate and removed efficiently by washout processes. As a result of the small concentration, the rate at which Cl_y/Br_y are transported to the stratosphere is expected to be small compared to the in situ stratospheric production. Thus, the transport of Cl_y/Br_y from the troposphere contributes little to the stratospheric concentration. In contrast, the origin of stratospheric Cl_y/Br_y from reactive source gases with tropospheric lifetimes comparable to the washout lifetime of Cl_y/Br_y (of order 10-30 days) in the troposphere is distinctly different. The in situ source in the stratosphere is expected to be significantly smaller because only a small portion of the source gas is expected to survive the troposphere to be transported into this region. At the same time, these short-lived source gases produce appreciable amounts of Cl_y/Br_y in the troposphere such that transport to the stratosphere offers a larger source for stratospheric Cl_y/Br_y than in situ production. Thus, for reactive source species, simple methods of estimating the concentration of stratospheric Cl_y/Br_y that ignore the tropospheric contribution will seriously underestimate the loading. Therefore, estimation of the stratospheric Cl_y/Br_y loading requires not only measurements of tropospheric source gases but also measurements of Cl_y/Br_y at the tropopause. We have further examined this mechanism by using results from a two-dimensional chemistry-transport model. However, in view of the importance of tropospheric transport on stratospheric loading, the detailed values should be further evaluated using a three-dimensional model with appropriate treatment of convective transport.

(2) Wamsley, P.R. et al. (1998), Distribution of halon-1211 in the upper troposphere and lower stratosphere and the 1994 total bromine budget, *J. Geophys. Res.* **103**, D1 1513-1526.

Stratospheric air was analyzed with a new gas chromatograph, flown aboard the NASA ER-2 aircraft as part of the Airborne Southern Hemisphere Ozone Experiment/Measurements for Assessing the Effects of Stratospheric Aircraft mission conducted in 1994. The mixing ratio of

SF_6, with its nearly linear increase in the troposphere, was used to estimate the mean age of stratospheric air parcels along the ER2 flight path. Measurement of H-1211 and mean age estimates were then combined with simultaneous measurements of CFC-11, measurements of brominated compounds in stratospheric whole air samples, and records of tropospheric organic bromine mixing ratios to calculate the dry mixing ratio of total bromine in the lower stratosphere and its partitioning between organic and inorganic forms. We estimate that the organic bromine-containing species were almost completely photolyzed to inorganic species in the oldest air parcels sampled. Our results for inorganic bromine are consistent with those obtained from a photochemical, steady state model for stratospheric air parcels with CFC-11 mixing ratios greater than 150 ppt. For stratospheric air parcels with CFC-11 mixing ratios less than 50 ppt (mean age $\geq$ 5 years) we calculate inorganic bromine mixing ratios that are approximately 20% less than the photochemical steady state model. There is a 20% reduction in calculated ozone loss resulting from bromine chemistry in old air relative to some previous estimates as a result of the lower bromine.

(3) Kotamarthi, V.R., J. M. Rodriguez, M.K.W. Ko, T.K. Tromp, N-D. Sze (1998), Trifluoroacetic acid from the degradation of HCFC and HFCs: a three dimensional modeling study, *J. Geophys. Res.* **103**, D5 5747-5758.

Trifluoroacetic acid (TFA) is produced by the degradation of the halcarbon replacements HFC-134a, HCFC-124, and HCFC-123. The formation of TFA occurs by HFC/HCFC reacting with OH to yield CF_3COX (X= F or Cl), followed by in-cloud hydrolysis of CF_3COX to form TFA. The TFA formed in the clouds may be re-evaporated but is finally deposited onto the surface by washout or dry deposition. Concern has been expressed about the possible long-term accumulation of TFA in certain aquatic environments, pointing to the need to obtain information on the concentrations of TFA in rainwater over scales ranging from local to continental. Based on projected concentrations of HFC-134a, HCFC-124, and HCFC-123 of 80, 10, and 1 pptv in the year 2010, mass conservation arguments imply an annually averaged global concentration of 0.16 µg/L if washout were the only removal mechanism for TFA. We present 3-D simulations of HFC/HCFC precursors of TFA that include the rates of formation and deposition of TFA based on assumed future emissions. An established (GISS/Harvard/UCI) but coarse-resolution (8° latitude by 10° longitude) chemical transport model was used. The annually averaged rainwater concentration of 0.12 µg/L (global) was calculated for the year 2010, when both washout and dry deposition are included as the loss mechanism for TFA from the atmosphere. For some large regions in the northern mid-latitudes, values are larger, 0.15-0.45 µg/L in parts of North America and Europe. Recent laboratory experiments have suggested that a substantial amount of

vibrationally excited CF3CHFO is produced in the degradation of HFC-134a, decreasing the yield of TFA from this compound by 60%. This decrease would reduce the calculated amount of TFA in rainwater in the year 2010 by 26%, for the same projected concentrations of precursors.

(4) Danilin, M.Y., N.D. Sze, M.K.W. Ko, J.M. Rodriguez, and A. Tabazadeh, (1998) Stratospheric cooling and Arctic ozone recovery, *Geophys. Res. Lett.*, **25** (12), 2141-2144.

Recent winter/spring observations in the Arctic reveal further reductions of the ozone content despite nearly complete disappearance of Pinatubo aerosol from the stratosphere and essentially constant levels of chlorine and bromine loading. Existing photochemical models of the stratosphere with heterogeneous chemistry predict little or no further stratospheric ozone depletion, unless an alternative mechanism is invoked. One such mechanism could be the cooling of the lower stratosphere leading to triggering of polar stratospheric cloud (PSC) formation. As a result, chlorine activation by enhanced PSCs provides further ozone decline during the winter/spring period. Here, we present sensitivity study results of the AER box model for typical conditions in the lower stratosphere at 70°N during the December 1 - April 1 period for an idealized parcel with different assumed stratospheric coolings and chlorine loadings. Our calculations show that the imposed stratospheric cooling could further deplete ozone and retard its expected recovery even with the projected chlorine loading decrease. We show that, for the present conditions, a 1 K cooling could provide the same local ozone depletion as an increase of chlorine by 0.40-0.95 ppbv for the scenarios considered. Thus, sustained stratospheric cooling could further reduce Arctic ozone content and delay the anticipated ozone recovery in the Northern hemisphere even with the realization of the Montreal Protocol and its Amendments.

(5) Shia, R-L, M.K.W. Ko, D. K. Weisentein, C. Scott, and J. Rodriguez, Transport between the tropical and mid-latitude lower stratosphere: Implication for ozone response to HSCT emissions, *J. Geophys. Res.*, in press

The subtropical barrier reduces the mixing between the tropics and the mid-latitudes in the lower stratosphere, and has significant effects on tracer distribution in the stratosphere. It is important for 2-D CTMs to have a realistic exchange rate between the tropics and mid-latitudes to simulate the effects of the subtropical barrier. The exchange rate is determined by the eddy diffusion coefficient K_{yy} in the model. In an earlier study, we introduced a tropical pipe by reducing the K_{yy} in the tropics from 0.3 to 0.03 (10^6 m^2/sec), (Weisenstein, et al. 1996). Recently, *in situ* measurements of chemical species with a wide range of local lifetimes have been used to quantify the air exchange rate between the tropics and mid-latitudes in the lower stratosphere from the tropopause to around 21 km. It is found that the mid-latitude air is entrained

into the tropical lower stratosphere with a replacement time scale of 10-18 months (Minschwaner et al., 1996; Volk et al., 1996). Meanwhile, Schoeberl et al. (1997) estimate the mixing time between the tropics and mid-latitudes in the 20-28 km region to be at least 18 months using the QBO signals in N_2O/CH_4 ratio and tropical winds from UARS measurements. These results demonstrate that the tropical barrier allows a moderate penetration.

The horizontal diffusion fluxes and the mixing ratio of CCl_4, CF_2Cl_2, $CFCl_3$, CH_3CCl_3, CH_4, HNO_3, N_2O, NO_y, and O_3 calculated in the AER 2-D model are used to derive the exchange rates between the tropics and the mid-latitudes in the lower stratosphere. They are compared with the exchange rates estimated from observations. Using the original model (global diffuser model) with a K_{yy} of 0.3 x 10^6 m^2/sec in the lower tropical stratosphere the model calculated exchange time scales are around 5-6 months. The tropical pipe model results show a much slower exchange rate of 38-60 months. Our studies showed that values for K_{yy} of 0.13 x 10^6 m^2/sec from the tropopause to 21 km and 0.07 x 10^6 m^2/sec from 21 km to 35 km in the model (leaky pipe model) will generate an exchange time scale of around 14 months below 20 km and 18 months in the 20-30 km region, in good agreement with the estimates from observations.

The model calculated lifetimes for species like N_2O and CFCs in the leaky pipe model are reduced by about 10% compared to the global diffuser model. Our model results show that the calculated ozone response to HSCT engine emissions is also smaller in the leaky pipe model.

(6) Ko, M.K.W., N.D. Sze, C. Scott, J.M. Rodriguez, and D.K. Weisenstein, (1998) Ozone depletion potential of CH3Br, *J. Geophys. Res.*, in press.

The ozone depletion potential (ODP) of CH_3Br is determined by combining the model calculated ODP/BLP ratio (where BLP is the bromine loading potential) for CH_3Br and its atmospheric lifetime. This paper examines how changes in several key kinetic data affect the ODP/BLP ratio. The key reactions highlighted in this study include the reaction of $BrO+HO_2$, the absorption cross-section of HOBr, the absorption cross-section and the photolysis products of $BrONO_2$, and the heterogeneous conversion of $BrONO_2$ to HOBr and HNO_3 on aerosol particles. By combining the calculated ODP/BLP ratio with the latest estimate of 0.7 year for the atmospheric lifetime of CH_3Br, the likely value of ODP for CH_3Br is 0.39. The model calculated concentration of HBr (~ 0.3 pptv) in the lower stratosphere is substantially smaller than the reported measured value of about 1.5 pptv. The model can reproduce the measured value of 1.5 pptv if one assumes a yield for HBr of 1.3% from the reaction of BrO+OH, or a yield of 0.6% from the reaction of $BrO + HO_2$. Our calculations show that the effect of these assumed rates on the model calculated ODP/BLP ratio is minimal: practically no impact for the assumed BrO+OH yield and 10% smaller for the $BrO+HO_2$ case.

Papers that have been submitted

(7) Danilin, M.Y., M.L. Santee, J.M. Rodriguez, M.K.W. Ko, J.M. Mergenthaler, J.B. Kumer, and A. Tabazadeh, Trajectory hunting: Analysis of UARS measurements showing rapid chlorine activation, submitted to *Geophys Res Lett.*

Trajectory hunting (i.e., a technique to find air parcels sampled at least twice over the course of a few days) is applied to analyze Upper Atmosphere Research Satellite (UARS) measurements in conjunction with the AER photochemical box model. In this study, we investigate rapid chlorine activation in the Arctic lower stratosphere on 29 Dec 1992 associated with a polar stratospheric cloud (PSC) event. Six air parcels that have been sampled twice were followed along 5-day trajectories at the 465~K (~46~mb) and 585 K (~22~mb) levels. A detailed sensitivity study with the AER photochemical box model along these trajectories leads to the following conclusions for the episode considered: (1) model results are in better agreement with UARS measurements at these levels if the UKMO temperature is decreased by at least 1-2 K; (2) the NAT (nitric acid trihydrate) PSC formation scheme produces results in better agreement with observations than the STS (supercooled ternary solution) scheme; (3) the model can explain the UARS measurements at 585 K, but underestimates the ClO abundance at 465 K, suggesting some inconsistency between the UARS measurements at this level.

(8) Danilin, M.Y., J.M. Rodriguez, W. Hu, M.K.W. Ko, D.K. Weisenstein, J.B. Kumer, J.L. Mergenthaler, J.M. Russell III, M. Koike, and G.K. Yue (1998), Nitrogen species in the post-Pinatubo stratosphere: Model analysis utilizing UARS measurements, submitted to *J. Geophys. Res.*

We present an analysis of the impact of heterogeneous chemistry on the partitioning of nitrogen species measured by the Upper Atmosphere Research Satellite (UARS) instruments. The UARS measurements utilized include: N_2O, HNO_3 and $ClONO_2$ (Cryogen Limb Array Etalon Spectrometer (CLAES), version 7), temperature, methane, ozone, H_2O, HCl, NO and NO_2 (HALogen Occultation Experiment (HALOE), version 18). The analysis is carried out for the data from January 1992 to September 1994 in the 100-1 mbar (~17-47 km) altitude range and over 10 degree latitude bins from 70°S to 70°N. Temporal-spatial evolution of aerosol surface area density (SAD) is adopted according to the Stratospheric Aerosol and Gas Experiment (SAGE) II data. A diurnal steady-state photochemical box model, constrained by the temperature, ozone, H_2O, CH_4, aerosol SAD and columns of O_2 and O_3 above the point of interest, has been used as the main tool to analyze these data. Total inorganic nitrogen (NO_y) is obtained by three different methods: 1) as a sum of the UARS measured NO, NO_2, HNO_3, and $ClONO_2$; 2) from the N_2O-NO_y correlation, 3)

from the CH_4-NO_y correlation. To validate our current understanding of stratospheric heterogeneous chemistry for post-Pinatubo conditions, the model-calculated NO_x/NO_y ratios and the NO, NO_2, and HNO_3 profiles are compared to the UARS-derived data. In general, the UARS-constrained box model captures the main features of nitrogen species partitioning in the post-Pinatubo years. However, the model underestimates the NO_2 content, particularly, in the 30-7 mbar (~23-32 km) range. Comparisons of the calculated temporal behavior of the partial columns of NO_2 and HNO_3 and ground based measurements at 45°S and 45°N are also presented. Our analysis indicates that ground-based and HALOE v.18 measurements of the NO_2 vertical columns are consistent within the range of their uncertainties and are systematically higher (up to 50%) than the model results at mid-latitudes in both hemispheres. Reasonable agreement is obtained for HNO_3 columns at 45°S suggesting some problems with nitrogen species partitioning in the model. Outstanding uncertainties are discussed.

(VII) References Cited

Shia, R.-L., M.K.W. Ko, D.K. Weisenstein, C. Scott, and J. Rodriguez, Transport between the tropical and mid-latitude lower stratosphere: Implication for ozone response to HSCT emissions, submitted to *J. Geophys. Res.*, 1998.

Volk, C.M., J.W. Elkins, D.W. Fahey, G.S. Dutton, J.M. Gilligan, M. Loewenstein, J.R. Podolske, K.R. Chan, and M.R. Gunson, Evaluation of source gas lifetimes from stratospheric observations, *J. Geophys. Res., 102*, 25543-25564, 199[illegible].

Butler, J.H., S.A. Montzka, A.D. Clarke, J.M. Lobert, and J.W. Elkins, Growth and distribution of halons in the atmosphere, *J. Geophys. Res., 103*, 1503-1511, 1998.

Kaye, J.A., S. Penkett, and F.M. Ormond, *Report on Concentrations, Lifetimes and Trends of CFCs, Halons, and Related Species, NASA Reference Publication 1339*, NASA Office of Mission to Planet Earth, Washington, D.C., 1994.

Gillotay, D., and P.C. Simon, Ultraviolet absorption spectrum of trifluoro-bromo-methane, difluoro-dibromo-methane and difluoro-bromo-chloro-methane in the vapor phase, *J. Atmos. Chem., 8*, 41-62, 1989.

Burkholder, J.B., R.R. Wilson, T. Gierczak, R. Talukdar, S.A. McKeen, J.J. Orlando, G.L. Vaghjiani, and A.R. Ravishankara, Atmospheric fate of CF_3Br, CF_2Br_2, CF_2ClBr, and CF_2BrCF_2Br, *J. Geophys. Res., 96*, 5025-5043, 1991.

DeMore, W.B., D.M. Golden, R.F. Hampson, M.J. Kurylo, C.J. Howard, A.R. Ravishankara, C.E. Kolb, and M.J. Molina, Chemical Kinetics and Photochemical Data for Use in Stratospheric Modeling, Evaluation No. 12, JPL Publication 97-4, Jet Propulsion Laboratory, Pasadena, 1997.

Minschwaner, K., R.W. Carter, and B.P. Briegleb, Infrared radiative forcing and atmospheric lifetimes of trace species based on observations from UARS, submitted to *J. Geophys. Res.*, 1998.

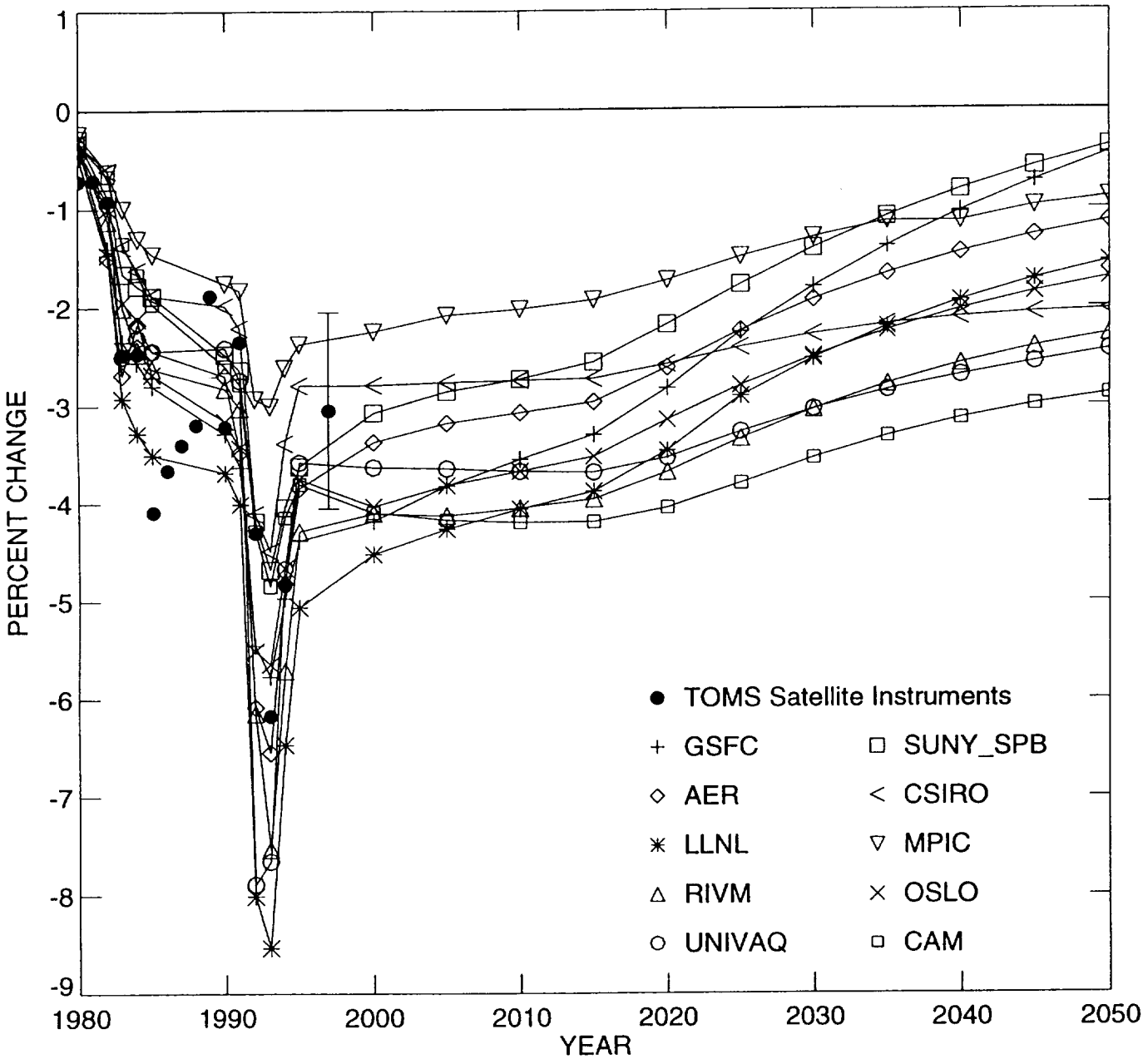

Figure 1: Percentage change in global (65S-65N) annual average column ozone, relative to 1979, between 1980 and 2050 as predicted by ten models for scenario A and A3 compared to observations from TOMS version 7 data (from Figure 12.9 of WMO 1998).

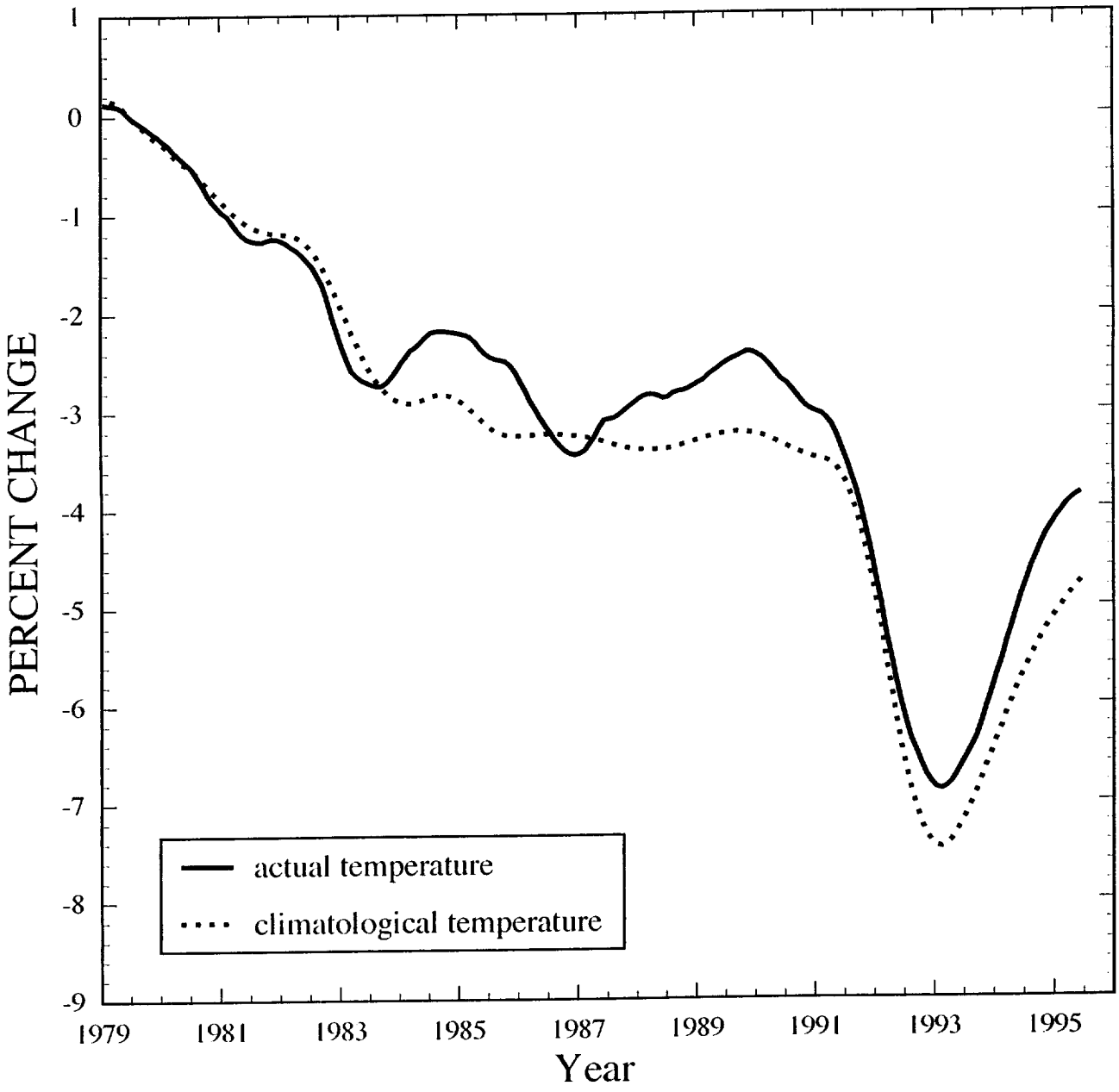

Figure 2: Percentage change in global (65S-65N) column ozone from the AER model using a 24-month running mean. The solid line represents an integration that includes the use of year-by-year mean temperatures and temperature probability distributions from NCEP. The dashed line uses the climatological temperature generated from 17 years of NCEP data (from Figure 12.7 of WMO 1998).

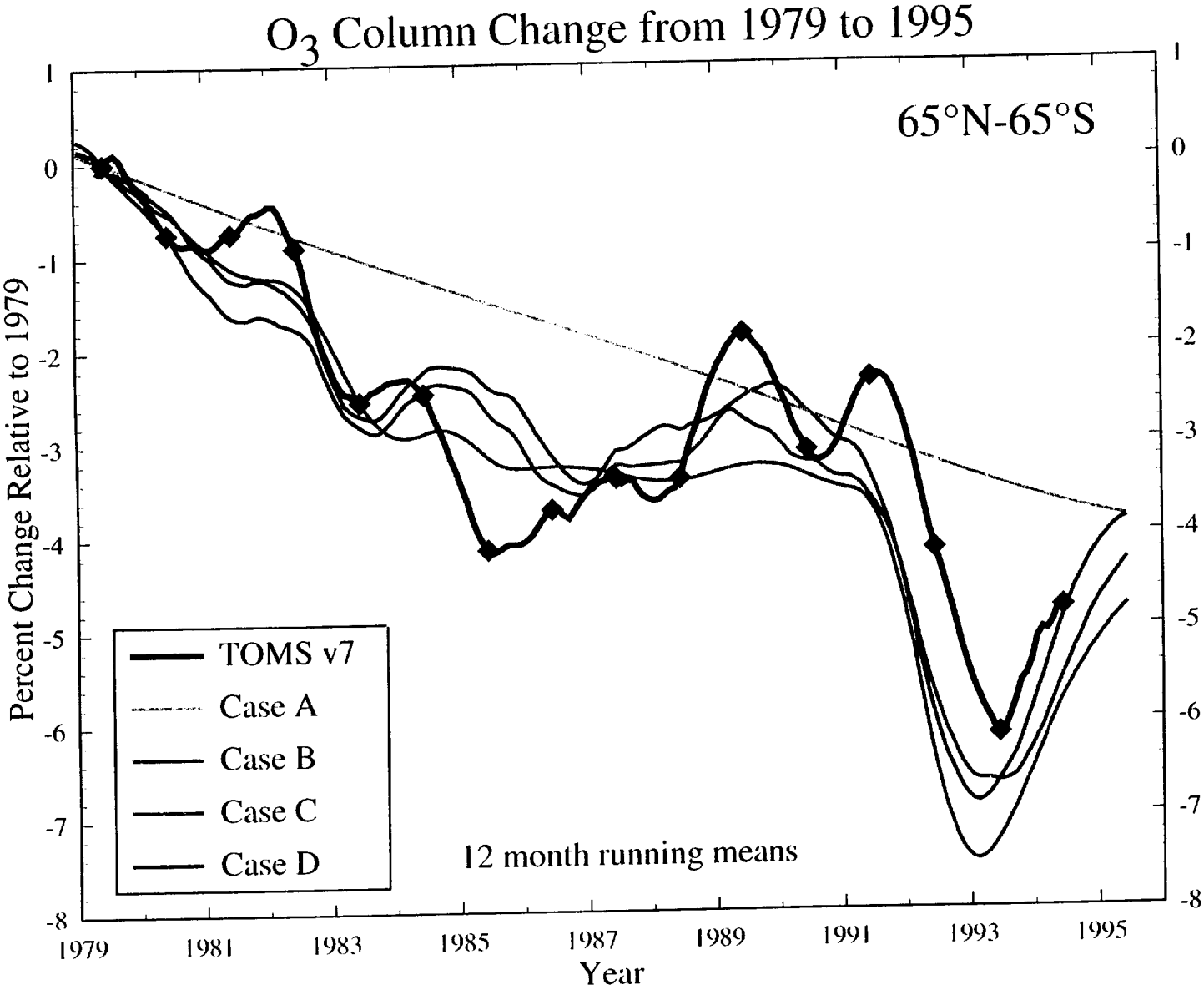

Figure 3: Pecent change in global (65S-65N) column ozone for 1979-1995 relative to 1979 from the AER model (Cases A-D) and TOMS version 7 using 12 months running means. Case A includes only trace gas increases. Case B includes trace gas increases and aerosol surface area variations. Case C includes trace gas increases, aerosol surface area variations, and zonal mean temperature variations. Case D includes trace gas increases, aerosol surface area variations, and variations in both the zonal mean and distribution of temperature.

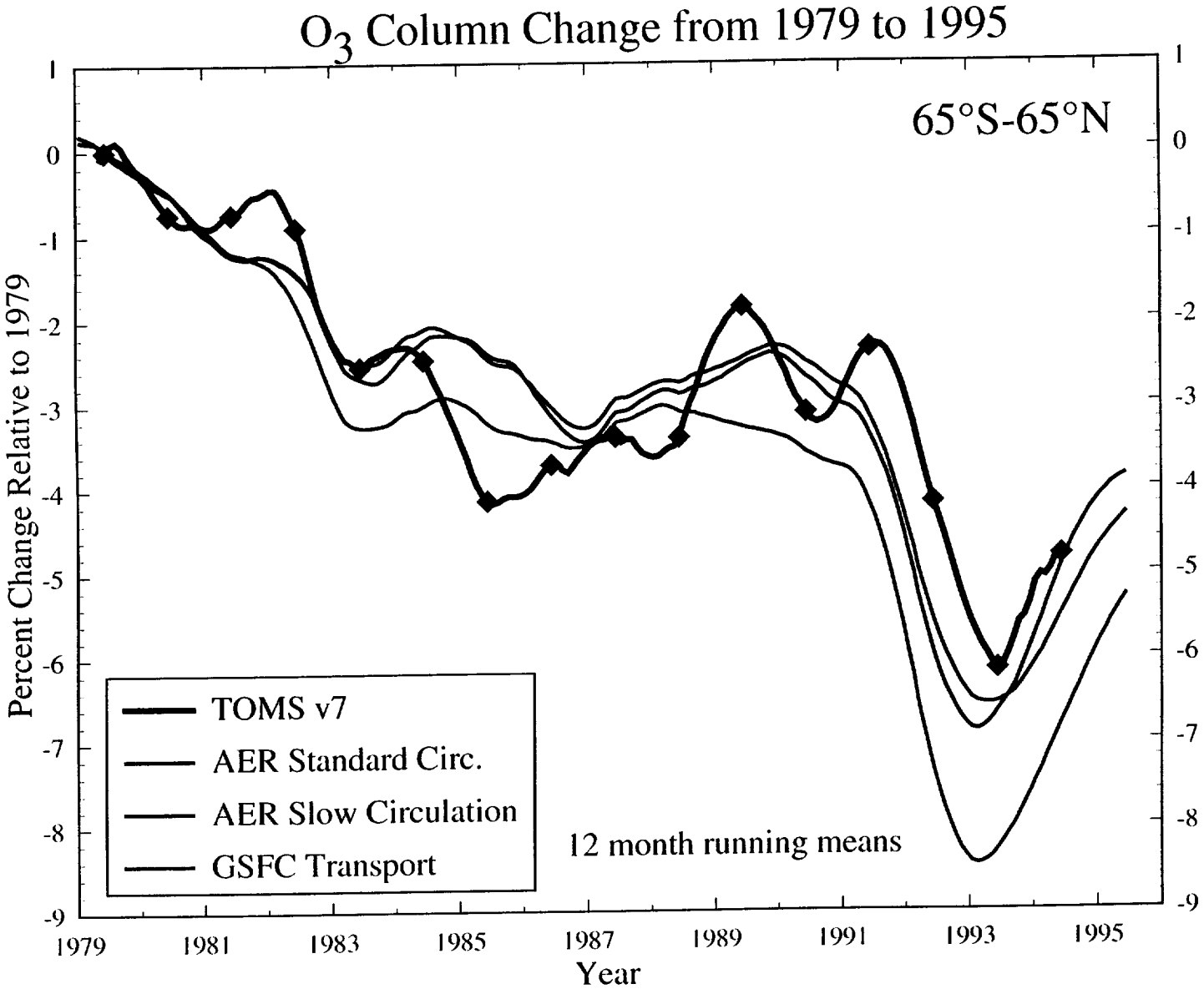

Figure 4: Pecent change in global (65S-65N) column ozone (12 months running means) for 1979-1995 relative to 1979 from the AER model with 3 different transport circulations. TOMS version 7 data are shown for comparison. The scenario includes trace gas increases, aerosol surface area variations, and variations in both the zonal mean and distribution of temperature.

APPENDIX A

"Calculation of Ozone Trends in the AER 2-D Model: Sensitivity to Interannual Temperature NASA Atmospheric Chemistry Modeling and Data Analysis Program Variations and Transport Barriers"

NASA Atmospheric Chemistry Modeling and Data Analysis Program

NAS5-97039: Semi-Annual Report on

Coupling Processes Atmospheric Chemistry and Climate

Paper Number A21A-05

Calculations of Ozone Trends in the AER 2-D Model: Sensitivity to Interannual Temperature Variations and Transport Barriers

Debra K. Weisenstein, Malcolm K.W. Ko,
Courtney J. Scott, and Run-Lie Shia

AER, Inc.
840 Memorial Dr.
Cambridge, MA 02139
Email: weisenstein@aer.com

AGU - Spring 1998

Description of AER 2-D Chemistry Transport Model

- Resolution: 9.5° latitude x 1.2 km
- JPL-97 chemistry with 5% branching of OH+ClO to HCl [Lipson et al., 1997]
- PSC Scheme
  - Thermodynamic equilibrium between gas phase and condensed HNO_3 and H_2O without supersaturation
  - Assumed NAT radius=0.5 μm, Ice radius=7 μm
  - Sedimentation and re-evaporation of solid HNO_3 and H_2O
- Temperature probability distribution [P(T)] used to account for deviations of temperature from monthly zonal mean
  - Used for all reactions rates
  - Used for PSC surface area calculation
  - Heterogeneous rates are $\Sigma P(T)\gamma(T)v(T)A(T)/4\ \Delta T$, ΔT=1 K

Calculated and Observed Ozone Column for 1979 (Dobson units)

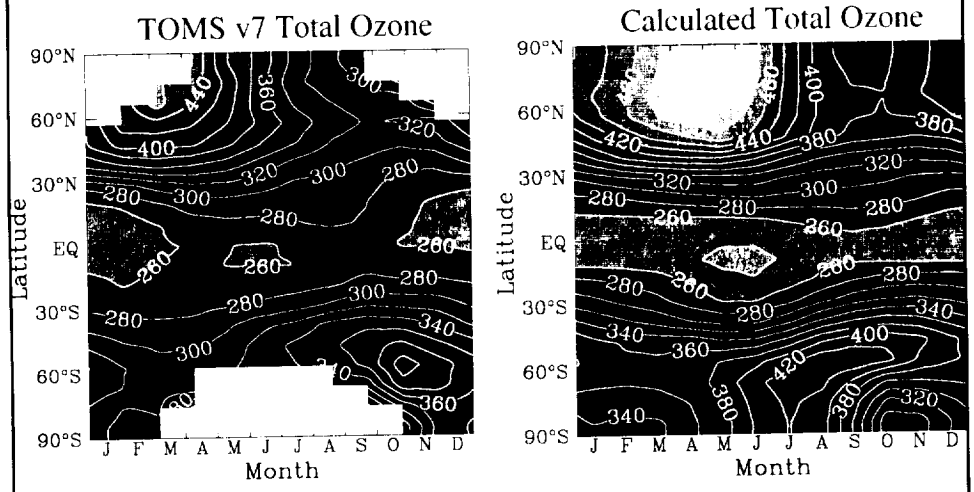

Description of Time-Dependent Ozone Calculation from 1970 to 1995

Case A: trace gas increases (ClY, BrY, N_2O, CH_4) [WMO 1998]
1979 aerosol surface area density (SAGE)
climatological temperatures (NCEP 1979-95)

Case B: trace gas increases +
aerosol surface area variations (SAGE, SAM, SME)

Case C: trace gas increases + aerosol surface area variations +
zonal mean temperature variations (NCEP)

Case D: trace gas increases + aerosol surface area variations +
zonal mean temperature variations +
variations in temperature probability distribution (NCEP)

- Model dynamics and solar flux fixed in all calculations
- TOMS version 7 data shown for comparison

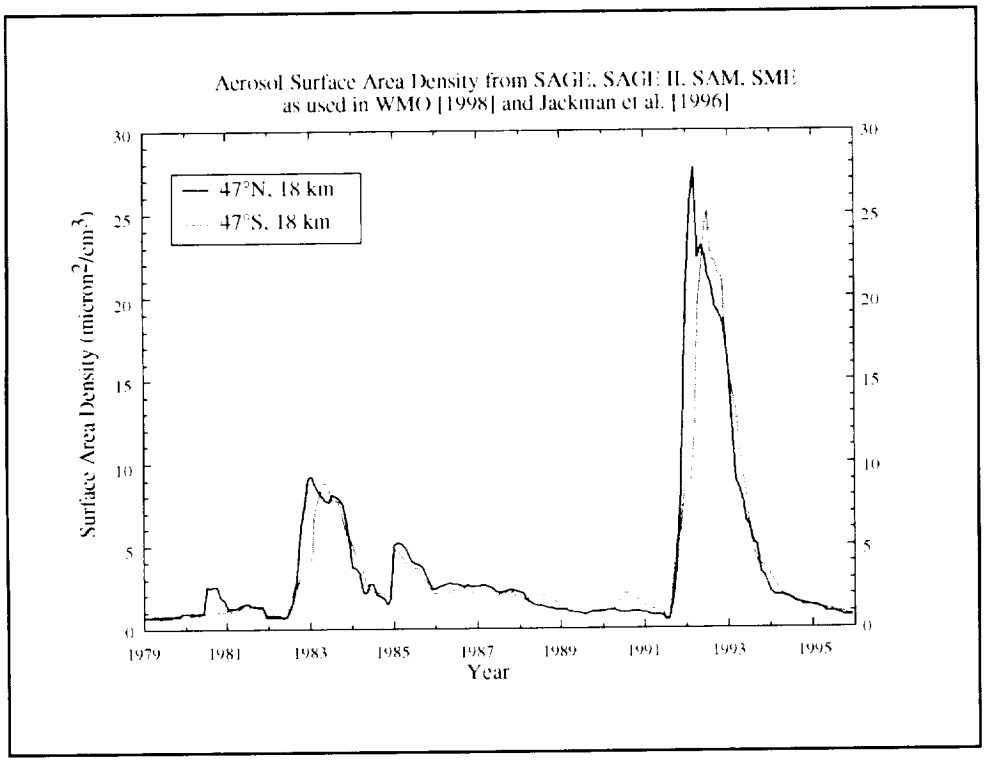
Aerosol Surface Area Density from SAGE, SAGE II, SAM, SME
as used in WMO [1998] and Jackman et al. [1996]
47°N, 18 km
47°S, 18 km
Surface Area Density (micron²/cm³)
Year
0
5
10
15
20
25
30
1979
1981
1983
1985
1987
1989
1991
1993
1995

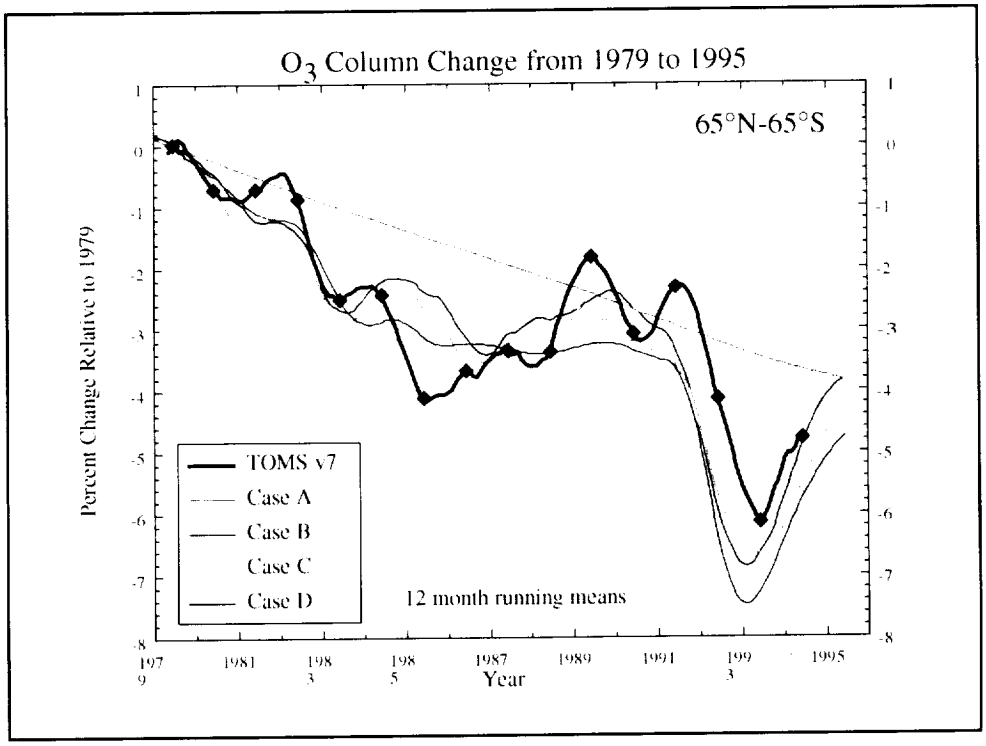
O_3 Column Change from 1979 to 1995
65°N-65°S
TOMS v7
Case A
Case B
Case C
Case D
12 month running means
Percent Change Relative to 1979
Year
1
0
-1
-2
-3
-4
-5
-6
-7
-8
1979
1981
1983
1985
1987
1989
1991
1993
1995

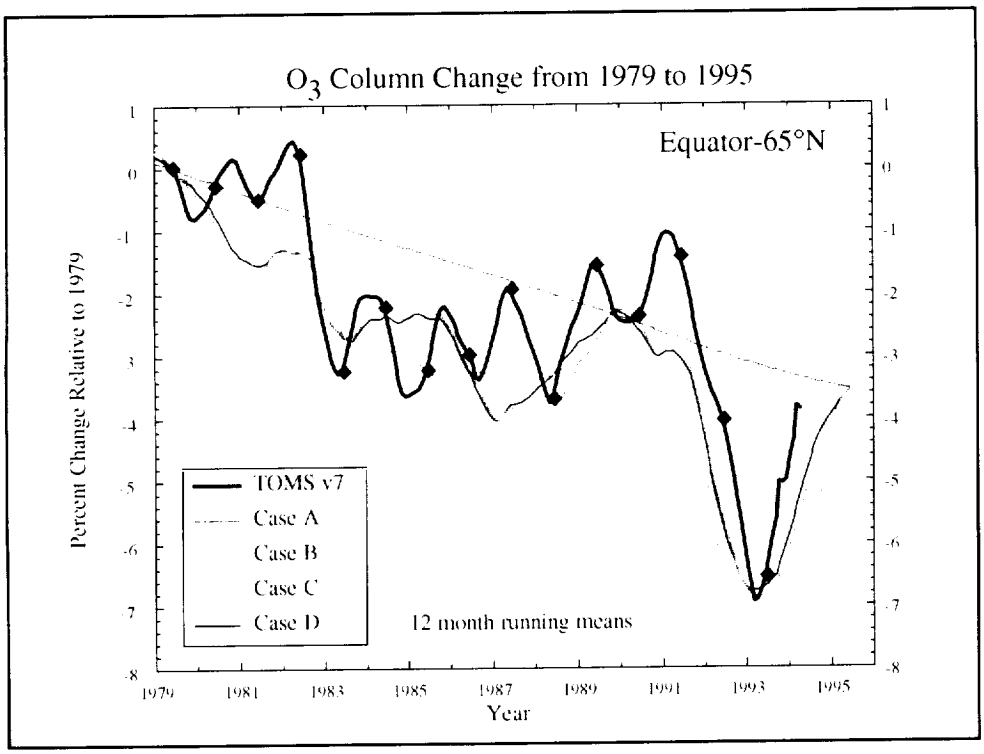
O_3 Column Change from 1979 to 1995
Equator-65°N
Percent Change Relative to 1979
Year
TOMS v7
Case A
Case B
Case C
Case D
12 month running means
1979
1981
1983
1985
1987
1989
1991
1993
1995

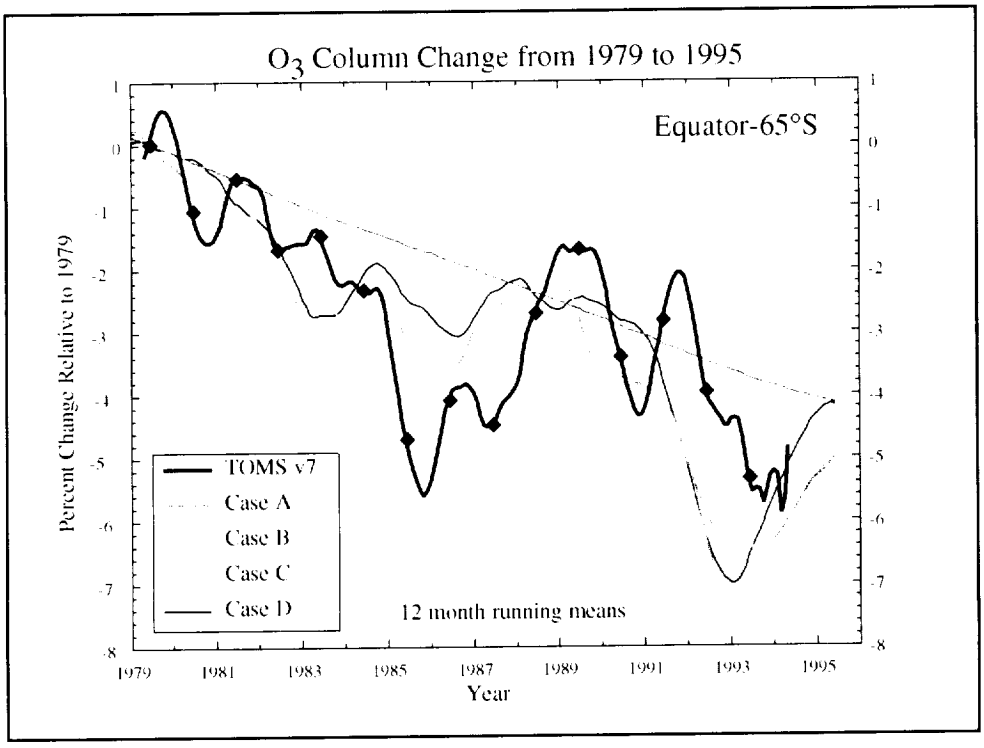
O_3 Column Change from 1979 to 1995
Equator-65°S
Percent Change Relative to 1979
Year
TOMS v7
Case A
Case B
Case C
Case D
12 month running means
1979
1981
1983
1985
1987
1989
1991
1993
1995

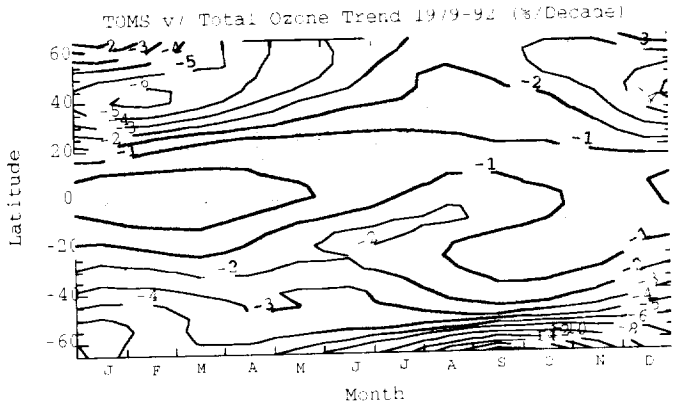

Case D Ozone Trend 1979-1992 (%/Decade from linear regression)

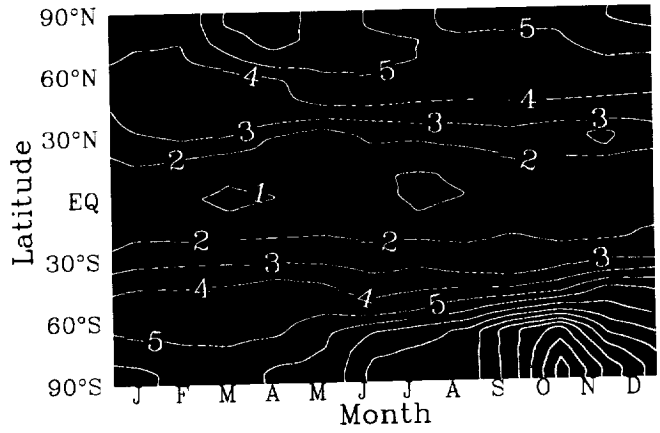

Case C Ozone Trend 1979-1992 (%/Decade from linear regression)

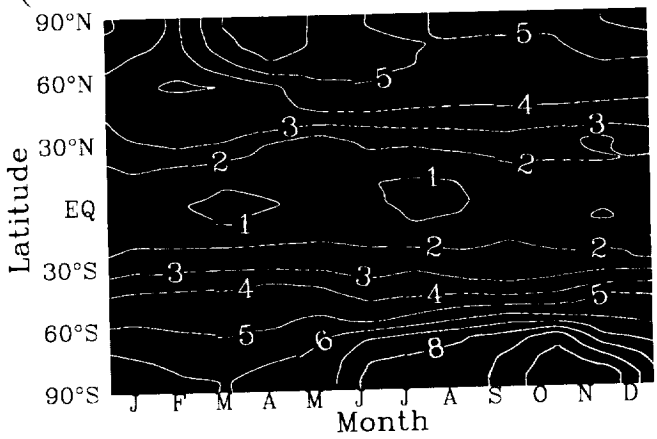

Case B Ozone Trend 1979-1992 (%/Decade from linear regression)

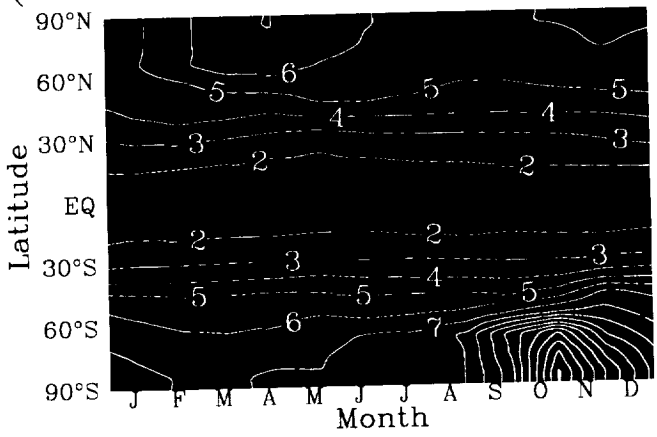

Case A Ozone Trend 1979-1992
(%/Decade from linear regression)

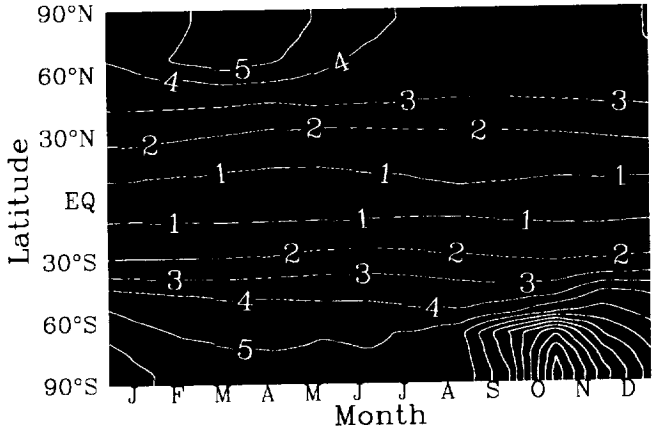

Ozone Trends for 1979-1992
(%/Decade from linear regression)

SBUV/SBUV-II

Case D

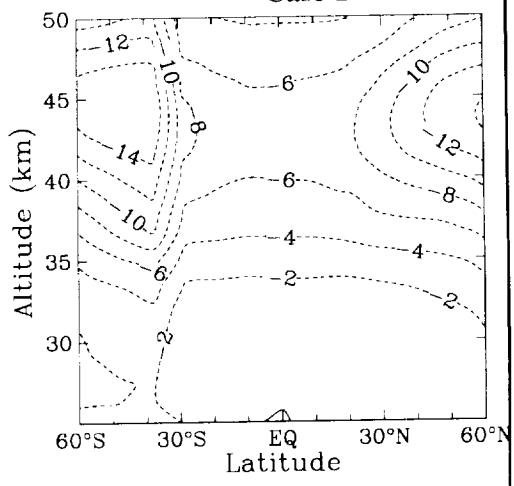

Figure 2 from Jackman et al. [1996]

Transport Issues and Sensitivity

- The transport in the AER 2-D model is known to be too vigorous, as demonstrated by low values of age-of-air relative to observations
- Sensitivity to transport formulation is demonstrated by repeating the "Case D" calculation with different transport formulations

Alternate Transport Formulations

- AER Slow Circulation: AER formulation with advective transport slowed by scaling streamfunction by factor of 0.6
- GSFC Transport: Transport formulation from NASA GSFC 2-D model [Jackman et al., 1996], based on climatological ozone and temperature fields.

Calculated Ozone Column for 1979 (Dobson units)

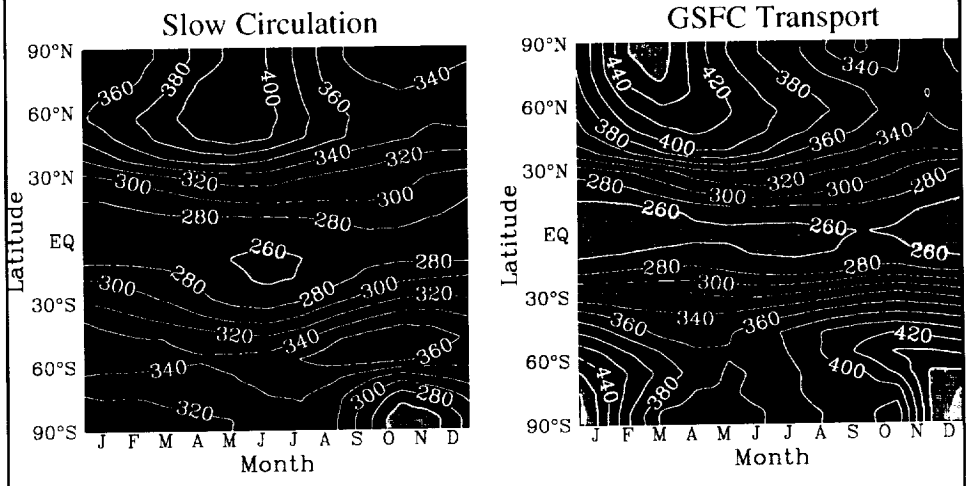

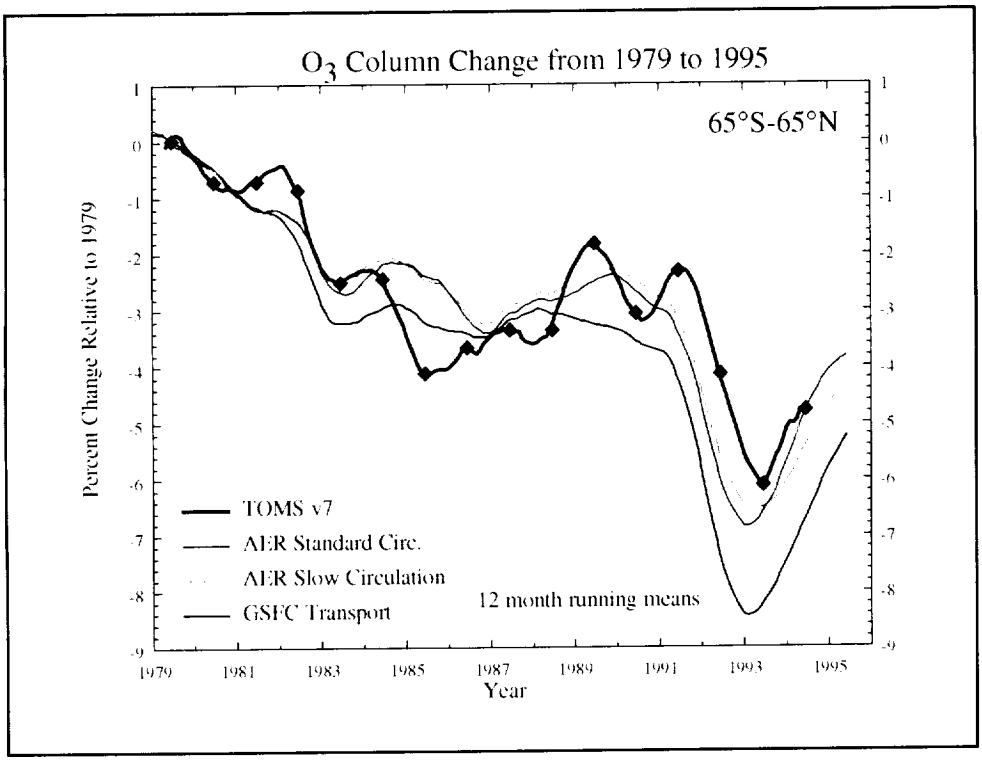
O_3 Column Change from 1979 to 1995
65°S-65°N
Percent Change Relative to 1979
TOMS v7
AER Standard Circ.
AER Slow Circulation
GSFC Transport
12 month running means
Year

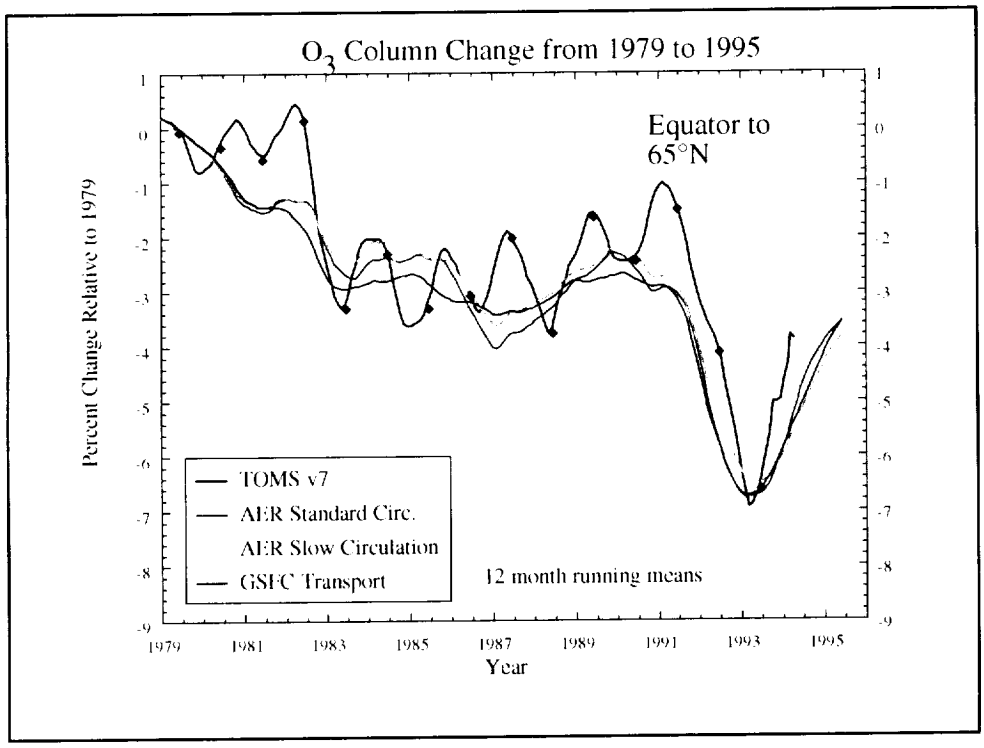
O_3 Column Change from 1979 to 1995
Equator to
65°N
Percent Change Relative to 1979
TOMS v7
AER Standard Circ.
AER Slow Circulation
GSFC Transport
12 month running means
Year

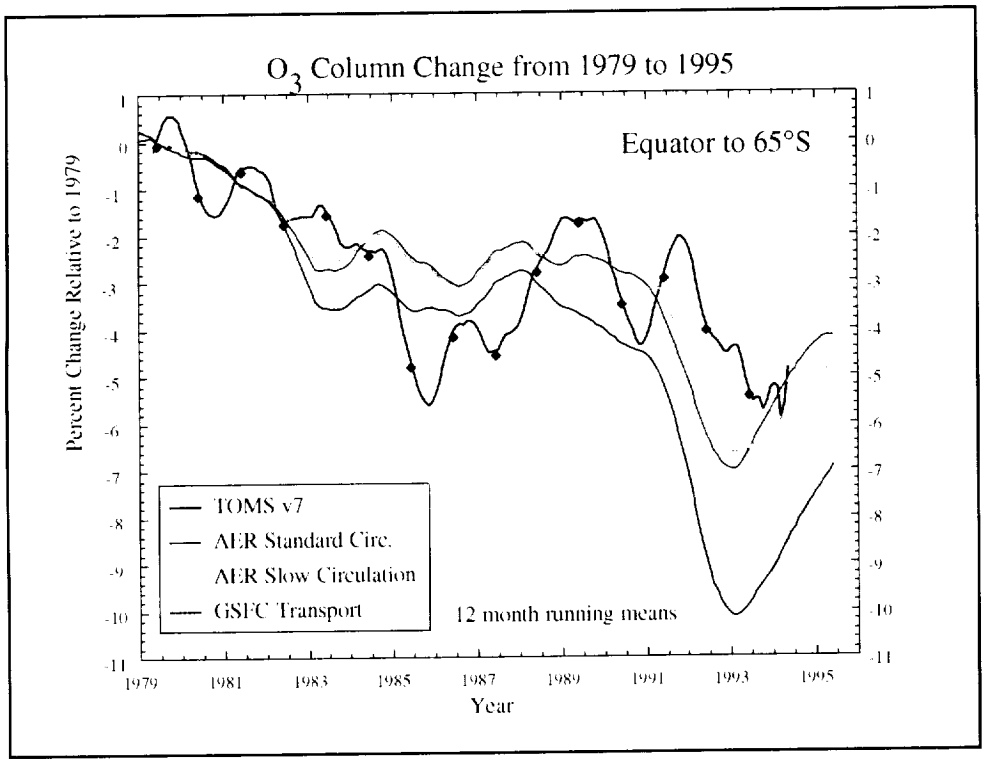
O_3 Column Change from 1979 to 1995
Equator to 65°S
Percent Change Relative to 1979
TOMS v7
AER Standard Circ.
AER Slow Circulation
GSFC Transport
12 month running means
1979
1981
1983
1985
1987
1989
1991
1993
1995
Year

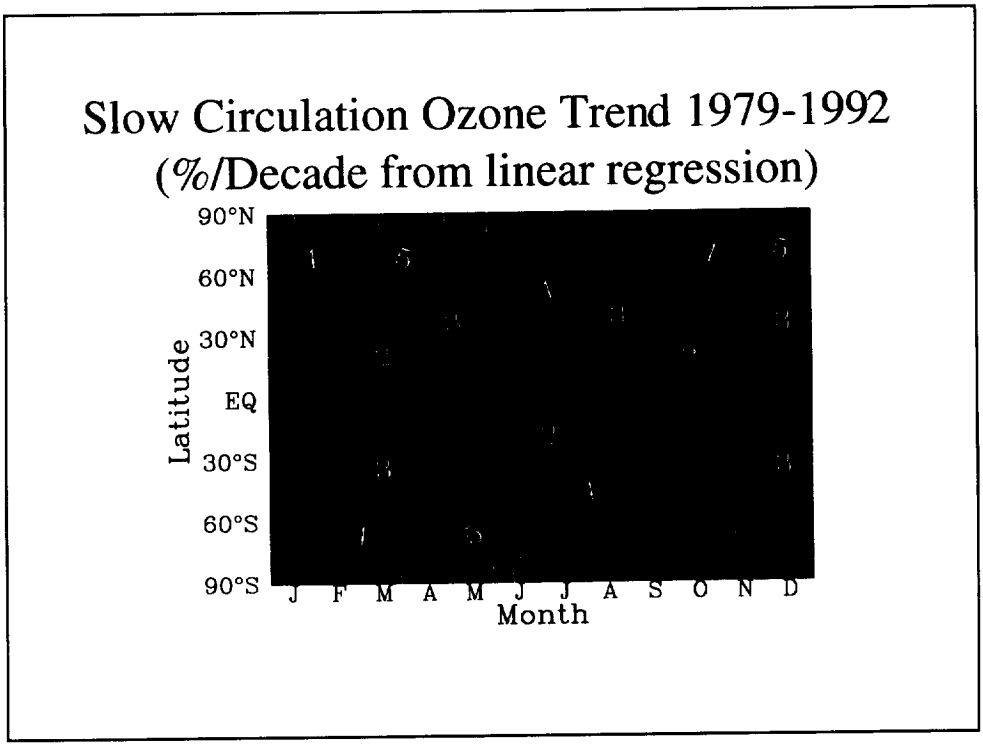
Slow Circulation Ozone Trend 1979-1992
(%/Decade from linear regression)
90°N
60°N
30°N
EQ
30°S
60°S
90°S
Latitude
J F M A M J J A S O N D
Month

GSFC Transport Ozone Trend 1979-1992
(%/Decade from linear regression)

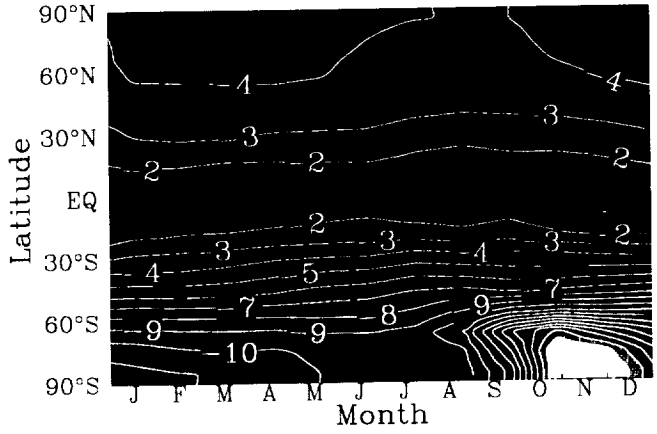

Ozone Trends for 1979-1992
(%/Decade from linear regression)

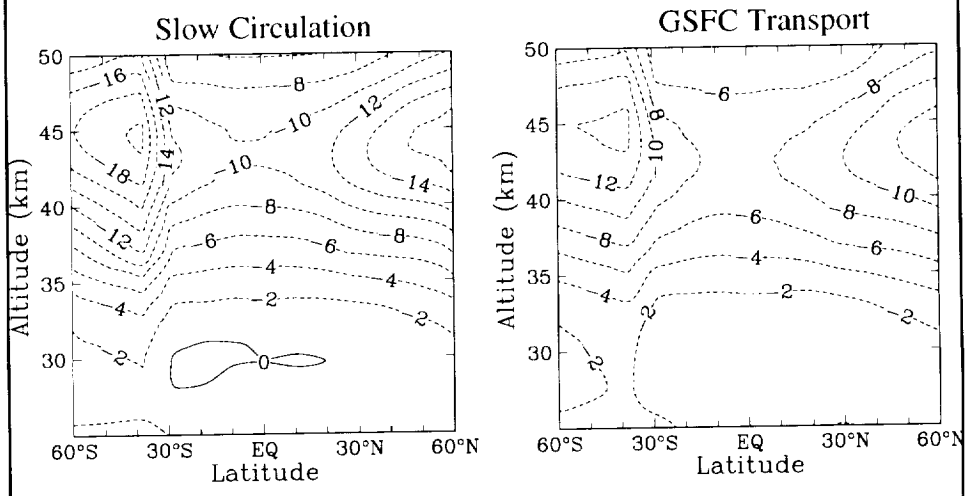

Discussion

- Sensitivity of ozone trends to aerosol variations has been previously noted by Solomon et al. [1996] and Jackman et al. [1996]
- Interannual variations in temperature are important to ozone trends, but dynamical variations may be equally important
- Climatological temperature probability distributions which include interannual as well as longitudinal temperature variations may be unrealistically broad
- AER model calculates excessive ozone trends in 35-50 km region, even with 5% branching of OH+ClO to HCl

References

Lipson, J.B., M.J. Elrod, T.W. Beiderhase, L.T. Moline, and M.J. Moline, Temperature dependence of the rate constant and branching ratio for the OH+ClO reaction, *J. Chem. Soc., Faraday Trans., 93*, 2665-2673, 1997.

Jackman, C.H., E.L. Fleming, S. Chandra, D.B. Considine, and J.E. Rosenfield, Past, present, and future modeled ozone trends with comparisons to observed trends, *J. Geophys. Res., 101*, 28753-28767, 1995.

Solomon, S., R.W. Portmann, R.R. Garcia, L.W. Thomason, L.R. Poole, and M.P. McCormick, The role of aerosol variations in anthropogenic ozone depletion at northern midlatitudes, J. Geophys. Res., 101, 6713-6727, 1996.

Solomon, S., R.W. Portmann, R.R. Garcia, W. Randel, F. Wu, R. Nagatani, J. Gleason, L. Thomason, L.R. Poole, and M.P. McCormick, Ozone depletion at midlatitudes: Coupling of volcanic aerosols and temperature variability to anthropogenic chlorine, *Geophys. Res. Lett., 25*, 1871-1874, 1998.

Weisenstein, D.K., M.K.W. Ko, N.D. Sze, and J.M. Rodriguez, Potential impact of SO_2 emissions from stratospheric aircraft on ozone, Geophys. Res., Lett., 23, 161-164, 1996.

Weisenstein, D.K., M.K.W. Ko, I.G. Dyominov, G. Pitari, L. Ricciardulli, G. Visconti, and S. Bekki, The effects of sulfur emissions from HSCT aircraft: A 2-D model intercomparison, *J. Geophys. Res., 103*, 1527-1547, 1998.

Acknowledgement: Special thanks to C.H. Jackman and E.L. Fleming for use of the GSFC 2-D model transport fields.

APPENDIX B

"Draft Section for Model and Measurement Workshop Report"

NASA Atmospheric Chemistry Modeling and Data Analysis Program

NAS5-97039: Semi-Annual Report on

Coupling Processes Atmospheric Chemistry and Climate

SOURCE GAS CHAPTER DRAFT

INTRODUCTION

Comparisons of measured and model calculated distributions and stratospheric lifetimes of long-lived source gases emitted from the surface of the earth provide a useful diagnostic for model transport and chemistry in the lower stratosphere. These long-lived species play an important role in the ozone budget, affecting the concentrations of Cly and Noy, which influence ozone production and loss. Source gases from the present day atmosphere were examined using calculations from participating models and selected measurements. These gases, unlike many of the tracers discussed in Part A, are dependent on chemistry as well as transport. Differences in chemical treatment among the models, such as photolysis rate calculations and diurnal averaging, could create substantial differences in source gas concentrations. A previous intercomparison of photolysis rates helped to remove much of the inter-model difference is this quantity, so we will assume that transport differences are responsible for the bulk of the inter-model differences in source gases. If this is true, then a consistent picture of model transport should emerge based both on source gases and the inert tracer experiments in Part A.

Observed source gas concentrations, which are compared with model results, are from the version 7.0 CLAES data from the UARS satellite, zonally averaged ATMOS data from the November 1994 ATLAS3 mission (Gunson et. al., 1996), and data from numerous aircraft campaigns that obtained *in-situ* measurements in the lower stratosphere between 1992 and 1997. Comparisons between measurements and model calculations can be difficult. Aerosols emitted during the Mt. Pinatubo eruption may have compromised CLAES data from 1991 and 1992. Aircraft campaigns do not always capture data representative of the zonal and climatological mean and do not take samples at many altitudes. Nevertheless, the measurements do provide a yardstick for model comparison.

Model results for source gases were obtained from Scenario B1, the 1992 atmosphere calculation. In this scenario, modelers were asked to calculate their best 1992 atmosphere. The models were initialized with a 1990 steady state calculation and then continued for an additional 2 years. Sulfate surface areas for 1991 and 1992 from SAGE II were provided, along with 1992 temperatures from NCEP. Models were required to use the JPL-97 reaction and photolysis rates (DeMore et. al, 1997). Models participating in this study were: AER, GSFC-2D,

LLNL, CSIRO, SUNY, UNIVAQ-2D, LARC-3D, HARVARD, GSFC-3D, ECHAM3/CHEM and NOCAR. Eight of the e even models provided both global and stratospheric calculated lifetimes for 10 source gas species, ranging from stratospheric lifetimes of 35 years for CH_3Br to around 200 years for $CHClF_2$. Close examination of mixing ratios, both in altitude and latitude, for CH_4, N_2O and $CFCl_3$ was also made. These particular species were selected based on the availability of measured data and their stratospheric lifetimes.

GLOBAL AND STRATOSPHERIC LIFETIMES

The atmospheric residence time, or lifetime, of a species defines the mixing ratio expected due to a given steady state emission rate. In our analysis, we examine the global lifetime, the total atmospheric burden divided by the total atmospheric loss, and the stratospheric lifetime, the total atmospheric burden divided by the stratospheric loss. Given the assumptions stated above, the global and stratospheric lifetimes of long-lived source gases may be useful in determining transport signatures within models. Global and stratospheric lifetimes for 10 species and eight models are shown in **Table 1.** For comparison, global lifetimes recommended in Scientific Assessment of Ozone Depletion (WMO, 1995) and stratospheric lifetimes derived from the ASHOE/MAESA (A/M) campaign (Volk et. al., 1997) are also shown. Note that for CF2Cl2, CFCl3, and CCl4, the derived mean stratospheric lifetime is smaller than the recommended global lifetime though the upper limit of the error range is comparable to the global lifetime. This may reflect the limited data used to derive the stratospheric lifetimes or uncertainty in the WMO global lifetimes.

The LARC model, the only 3D CTM to submit lifetimes, calculates stratospheric lifetimes for N_2O, CF_2Cl_2, and CH_3Cl that are substantially longer than the other models and 40% longer than the derived stratospheric lifetimes from A/M. Comparison of LARC with the WMO global lifetimes also indicate the 3D CTM is calculating more than 40% longer lifetimes for N_2O and CF_2Cl_2. It should be noted that the unusually large lifetimes calculated by the LARC model may be due to a non-converged 1990 data set.

Comparison of the global lifetimes with the WMO lifetimes for the longer lived species, N_2O, CF_2Cl_2 and $C_2Cl_3F_3$, indicate the remaining seven models calculate lifetimes in good agreement with the documented values, calculating mean global lifetimes that are within +/-5% of the WMO values. The calculated global lifetimes of the shorter lived species show model means, with the exception

of the HARVARD model which calculates much longer OH reactive lifetimes than any of the other models, to be within +/-10% of the WMO values for the OH reactive species and within +/-25% for the photolytically reactive species.

Comparison of the calculated stratospheric lifetimes for the long-lived species, N_2O, CF_2Cl_2 and $C_2Cl_3F_3$, show most of the models to be in good agreement with the A/M lifetimes, calculating mean lifetimes within the error bars noted. For N_2O and CF_2Cl_2, the LARC value is close to a factor of 2 larger than the A/M value. While the rest of the models are within +/- 10% of each other, around 100 years. Among the seven models, AER and LLNL calculate the shortest lifetimes while GSFC calculates the longest. All of the models calculate much longer lifetimes for CH_4 than the A/M values indicate. The calculated lifetimes of the short-lived species do not represent the derived values as well as the long-lived species. For $CFCl_3$, GSFC, HARVARD and LARC calculate lifetimes around 60 years, about 50% larger than the A/M value. The remaining five models calculate a mean lifetime within +/- 10% of each other around 47 years, well within the error bars noted. HARVARD and GSFC calculate lifetimes larger than 55 years for CCl_4, about 70% larger than the A/M values. Values from the remaining six models calculate a mean of 44 years, very close to the A/M calculated values. In this group, the UNIVAQ-2D calculates the shortest lifetimes closest to the A/M lifetimes.

The 10 species studied can be separated into two groups, those with stratospheric lifetimes less than 60 years and those with stratospheric lifetimes over 120 years. Species with shorter lifetimes such as CCl_4 and $CFCl_3$ are more sensitive to the transport characteristics at 75 mb while those with longer lifetimes (such as N_2O and CF_2Cl_2) are more sensitive to the model transport around 10 mb. The 2D CTMs are in relatively good agreement with each other. In **Figure 1**, patterns can be noted with certain models. The HARVARD model tends to calculate lifetimes that are shorter for the longer lived species, while they calculate large lifetimes for the shorter lived species we examined. The UNIVAQ-2D model shows an opposite pattern, where the shorter lived species have lifetimes below the mean of all models. The remaining models tend to be in the middle and show no obvious patterns. These behaviors apply to species whose removals are both driven by photolysis and by OH chemistry and is interpreted as indicative of the transport differences in the models. A general pattern is noted that models that tend to calculate shorter lifetimes for a given species have steeper latitudinal gradients for that species. This behavior may be indicative of the strength of the tropical

upwelling and/or the tropical barrier. Comparison of the model calculated stratospheric lifetimes shows AER and LLNL tend to calculate similar lifetimes. Based on these correlations, AER and LLNL may have similar upwelling and/or have similiar tropical barriers at the 75 and 10 mb surfaces. HARVARD and UNIVAQ-2D may have smaller upwelling rates at their 75 mb surface. The differences in model calculated lifetimes seem to be related to the age of air from the SF_6 and the tracer experiments, see pertinent sections. Models that are calculating longer lifetimes tend to have older air, giving model calculated ages that are closer to the age of air derived from measurements of SF_6 (Volk et. al., 1997) and CO_2 from the ER-2 aircraft. The longer source gas lifetimes in the models could suggest that the upwelling in the lower tropical stratosphere for the models is too weak but this is inconsistent with the findings from the CO_2 study, which deduces that the model calculated seasonal signal for CO_2 is advected up in the tropics too fast when compared to observations. This seemingly contradictory situation, that the model ages are too young from the SF_6 experiment, but the model calculated lifetimes are too long compared to observations, could be an indication that the meridional flux across the tropical barrier is too weak.

SOURCE GAS CONCENTRATIONS

In order to discern dynamical signatures of upwelling verses horizontal mixing in the lower stratosphere, results from the AER 2-D CTM using three different mixing rates ranging from a weak tropical barrier to a strong tropical barrier were examined. The models are: the Global Diffuser (NO-PIPE) (Kotamarthi et al., 1994; Weisenstein, et al., 1993); the Partial Barrier (LEAKY-PIPE) (Shia et. al., 1996); and the Tropical Barrier (PIPE) (Weisenstein et. al., 1996). The three models have identical chemistry and advection and differ only in the horizontal diffusion coefficient in the lower and middle stratosphere. Three different properties of the source gases were examined: lifetimes, latitudinal cross sections at specified altitudes, and profiles at specified latitudes. **Table 2** illustrates stratospheric calculated lifetimes for the three AER models. In all species examined, the PIPE model calculates the youngest lifetimes while the NOPIPE model calculates the oldest lifetimes. This is true not only for the photolytically driven species, but also for the OH reactive species, such as CH_4. Clearly, the strength of the tropical barrier effects the lifetimes of the species, as the highest concentrations are found in the tropical regions where chemical processing is most intense. Thus, the highest concentrations are seen with the

strongest tropical barriers, leading to greater overall loss and shorter lifetimes. Differences in advective transport may also impact the permeability of the tropical barrier. If this is truly a transport signature, the calculated species concentrations in the tropics should be correlated with lifetimes. Specifically, models which calculate longer lifetimes should also calculate smaller concentrations in the lower tropical stratosphere. Additionally, one expects the gradients of the source gas isopleths to be steeper across the tropical barrier if the model is calculating shorter lifetimes. To test this hypothesis, three source gas species were examined: CH_4 and N2O at 10 mb and $CFCl_3$ at 75 mb. **Figure 2** shows the latitudinal cross sections at 10 mb of spring calculated CH_4 for all models. In figure 2, GSFC, UNIVAQ-2D, SUNY, LARC and GSFC-3D are all grouped together peaking 20% below the zonal mean UARS CH_4 in the tropics. The remaining models, AER, HARVARD, LLNL, NOCAR and CSIRO, all fall within 10% of the UARS zonal mean CH_4 in the tropics. Spring and fall equatorial profiles of CH_4 for all models, UARS and ATMOS are shown in **Figure 3.** In the lower stratosphere all model calculated CH_4 falls below the measured UARS data. Note that the ATMOS data is lower in magnitude and the models are higher than ATMOS data for the same altitude range. A large spread is seen in calculated CH_4 concentrations in the middle and upper stratosphere.

Figure 4 shows the latitudinal cross section of spring N_2O at 10 mb. As in **figure 2**, UARS zonal mean data are shown for 1992 and 1993. Much larger variation is seen in the UARS N_2O data than in the CH_4 data. This may be due to a small contamination by the Mt. Pinatubo aerosols effecting the data retrieval. Again, the models fall into two separate groups. The first group, containing the models SUNY, LARC, UNIVAQ-2D and GSFC-3D, are approximately 10% below the UARS tropical concentrations. The second group, consisting of the models AER, HARVARD, LLNL, NOCAR and CSIRO range from between 15 to 40% to high in the tropics. The GSFC-2D model falls the closest to the UARS data. **Figure 5** shows spring and fall equatorial profiles for N_2O. In contrast to the CH_4, the calculated N_2O values more closely represent the UARS and ATMOS measured N_2O in the lower stratosphere, falling within +/- 30%. The spread in the middle and upper stratosphere is as large for the N_2O as the CH_4.

Figures 6 and 7 show fall $CFCl_3$ calculated and measured data, with a latitudinal cross section at 75 mb and an equatorial profile, respectively. Examination of **Figure 6** does not show the same pattern that both the N_2O and CH_4 at 10 mb did. This is indicative of a different pattern of mixing that drives the

Calculated species cross sections of N_2O and CH_4 show larger gradients across the tropical barrier than the UARS data would indicate. This also substantiates mixing ratios that are too high and ages of air that is to young. Conversely, measured data from the ATMOS and ER-2 flights for $CFCl_3$ indicate a larger gradient at the 75 mb region than the models are exhibiting. This indicates the models may have to much meridional mixing at the 75 mb level. Clearly, the transport in the models differs for each altitude examined and obtaining more realistic transport will not be trivial. Additionally, a large spread of calculated mixing ratio values is seen for all species examined at high latitudes. This may be indicative of different polar process or differences in high latitude dynamics. These differences should be considered when interpreting results concerning the HSCT impact on ozone.

REFERENCES

DeMore, W.B, et al., Chemical Kinetics and Photochemical Data for Use in Stratospheric Modeling, JPL Publication 97-4, 1997.

M. R. Gunson et al. "The atmospheric trace molecule spectroscopy (ATMOS) experiment: Deployment on the ATLAS Space Shuttle missions" GRL 23, pp 2333-2336 (1996).

Kotamarthi, V.R., M.K.W. Ko, D.K. Weisenstein, J.M. Rodriguez, and N.D.Sze, Effect of Lightning on the concentration of odd nitrogen species in the lower stratosphere: An update, *J. Geophys. Res.*.,99, 8167-8173,1994.

Volk, C.M, Elkins, J.W., Fahey, D.W., Dutton, G.S., Gilligan, J.M., Loewenstein, M., Podolske, J.R., Chan, K.R., Gunson, M.R., Evaluation of source gas lifetimes from stratospheric observations, *J. Geophys. Res.*, **102**, 25,543 - 25,564, 1997.

Shia, R.-L., M. K. W. Ko, D. K. Weisenstein, C. Scott and J. Rodriguez, Transport between the tropical and mid-latitude lower stratosphere: Implications for ozone response to HSCT emissions, J. Geophys. Res., submitted, 1997.

Weisenstein, D.K., Ko, M.K.W., Sze, N.D. and Rodriguez, J.M., Potential impact of SO_2 emissions from stratospheric aircraft on ozone, *Geophys. Res. Lett.*, **23**, 161-164, 1996.

Weisenstein, D.K., M.K.W.Ko, J.M. Rodriguez, and N.D. Sze, Effects on statospheric ozone from high-speed civil transport: Sensitivity to stratospheric aerosol loading, *J. Geophys. Res..*, 98, 23133-23140, 1993

World Meteorological Organization (WMO), Scientific assessment of ozone depletion:1994, Rep. 37, Global Ozone Res. and Monit. Project., Geneva, 1995

Table 1: Calculated Global and Stratospheric lifetimes in years for participating models and measurements. The global lifetime is the upper value.

	LARC	HARVARD	GSFC-2D	SUNY	UNIVAQ-2D	CSIRO	LLNL	AER	
SPECIES									
N_2O	174.76 177.66	121.60 122.30	130.00 132.06	124.78 125.58	122.28 122.77	116.90 117.80	105.83 107.10	109.08 109.79	120@ 124 +/-49**
CF_2Cl_2	148.80 151.48	92.17 106.40	111.20 112.32	106.45 107.15	104.55 104.97	100.10 100.80	92.17 93.37	92.17 92.71	102 77 +/- 26
$C_2Cl_3F_3$	- -	54.87 58.60	101.40 102.57	86.66 87.44	81.32 81.69	82.47 83.35	80.60 81.39	76.55 77.16	85 89 +/- 35
$CFCl_3$	57.36 59.28	67.74 70.22	61.44 62.89	48.83 49.72	43.83 43.99	53.41 54.64	49.30 51.06	47.43 48.19	50 41 +/- 12
CCl_4	43.91 45.41	64.12 66.87	53.26 55.19	38.83 40.00	36.25 36.43	45.50 47.22	41.96 44.01	40.76 41.76	42 32 +/- 11
CH_4	- -	26.46 156.50	8.68 167.97	12.73 163.87	11.03 166.18	11.02 155.00	12.17 139.90	11.92 127.86	14.5 84 +/- 35
CH_3Cl	1.43 114.90	4.42 64.51	1.39 77.38	2.01 65.30	1.81 57.96	1.75 57.01	1.91 51.78	1.95 58.82	- -
CH_3CCl_3	4.96 48.56	14.04 63.68	4.86 56.02	6.61 42.37	5.87 37.19	2.14 47.29	6.39 42.69	6.40 41.72	5.4 30 +/- 9
CH_3Br	1.73 37.80	5.86 54.22	1.71 48.12	2.41 33.86	2.08 28.80	6.01 37.91	2.33 37.19	2.35 35.07	1.7* -
$CHClF_2$	- -	34.87 209.80	11.78 309.34	16.47 135.16	14.59 205.77	14.62 206.30	16.00 222.52	15.92 197.10	13.3 -

@ denotes the global lifetimes from the WMO 1995 report, Table 13-1.

** stratospheric lifetimes are given by Volk et. al. 1997 calculations based on ASHOE/MAESA measurements.

* denotes the global lifetime from the WMO 1995 report, Chapter 10.

Table 2: Calculated stratospheric lifetimes in years of the AER 2-D CTM with different mixing rates in the tropical and sub-tropical region

	NOPIPE	**LEAKY PIPE**	**PIPE**
SPECIES			
N_2O	132.18	110.19	103.20
$C_2Cl_3F_3$	94.94	77.65	72.43
$CHClF_2$	224.27	204.99	200.58
$CFCl_3$	57.62	48.68	45.92
CF_2Cl_2	113.59	93.26	87.00
CCl_4	49.16	42.23	40.10
CH_3Cl	72.51	63.30	61.86
CH_3Br	40.79	35.95	34.72
CH_3CCl_3	49.26	42.41	40.41
CH_4	150.98	132.99	127.90

Figure 1: Graphical representation of the Model calculated stratospheric lifetimes (years) shown in Table 2. Species in the upper half of the figure are primarily driven by photolytic reactions while species below the dotted line are driven primarily by the OH reaction.

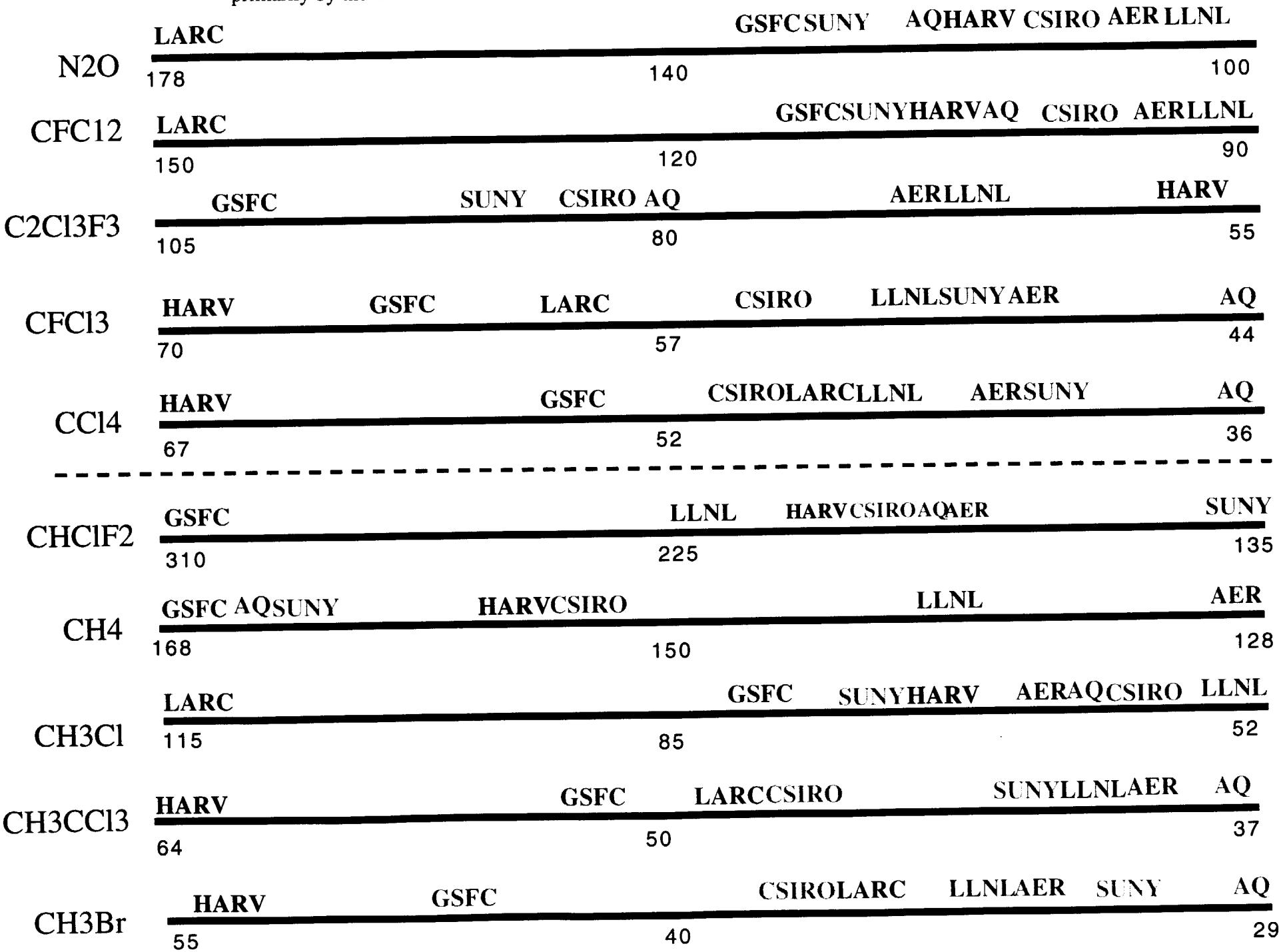

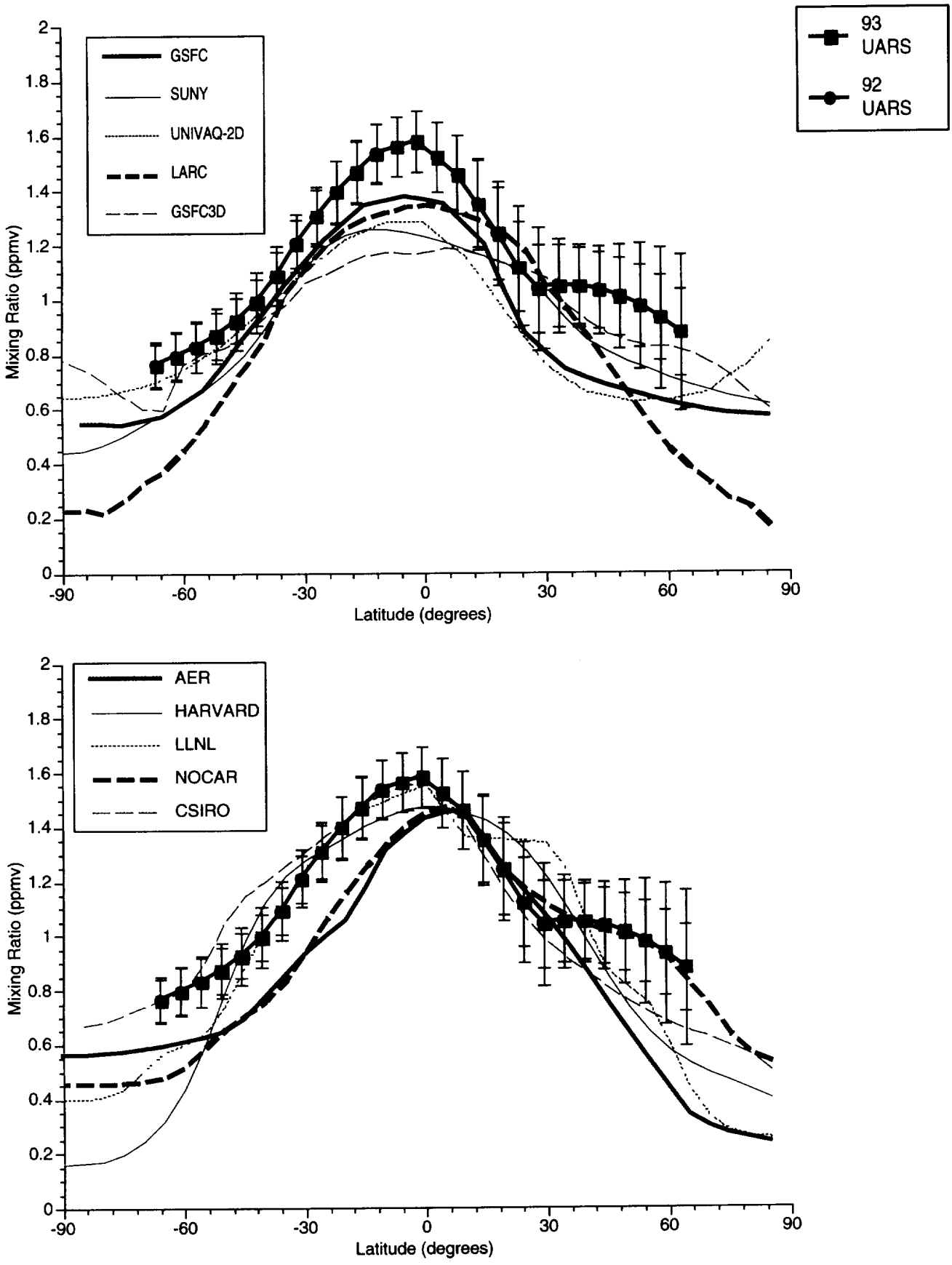

Figure 2: Calculated CH4 for spring at 10 mb. Symbols denote the spring 10 mb UARS version 7.0 CLAES data. Error bars represent the meridional variations of the CH4.

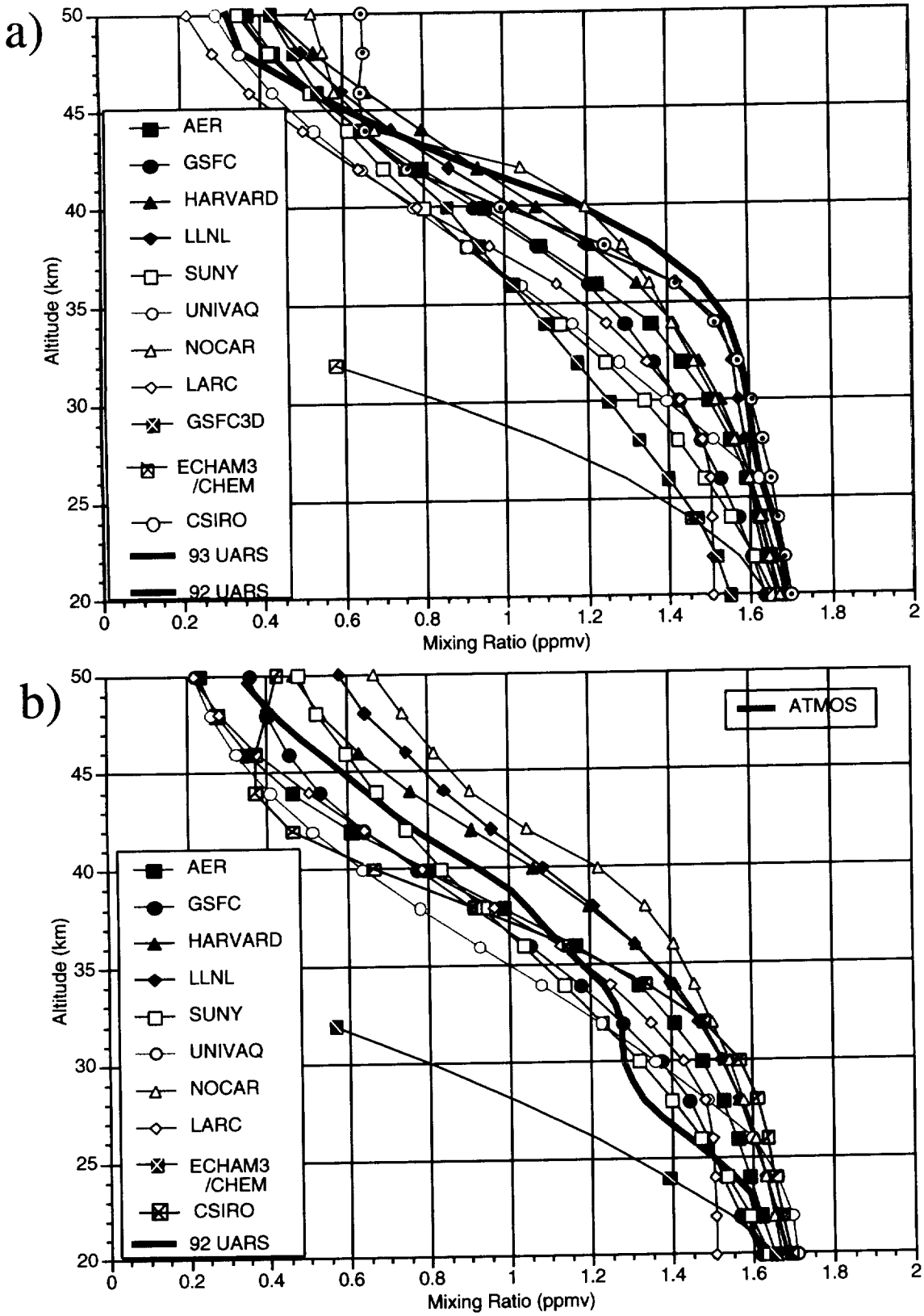

Figure 3: Calculated CH4 at the equator between 20 and 50 km. Spring data is in the upper panel (a) while fall values are given in the lower panel (b). Solid lines denote UARS and ATMOS data. The ECHAM3/CHEM calculated points represent the model's resolution. Values are shown at 20, 24 and 32 km. The 32 km value represents the top layer of the model, from 0 hPa to 20 hPa and centered at 10 hPa.

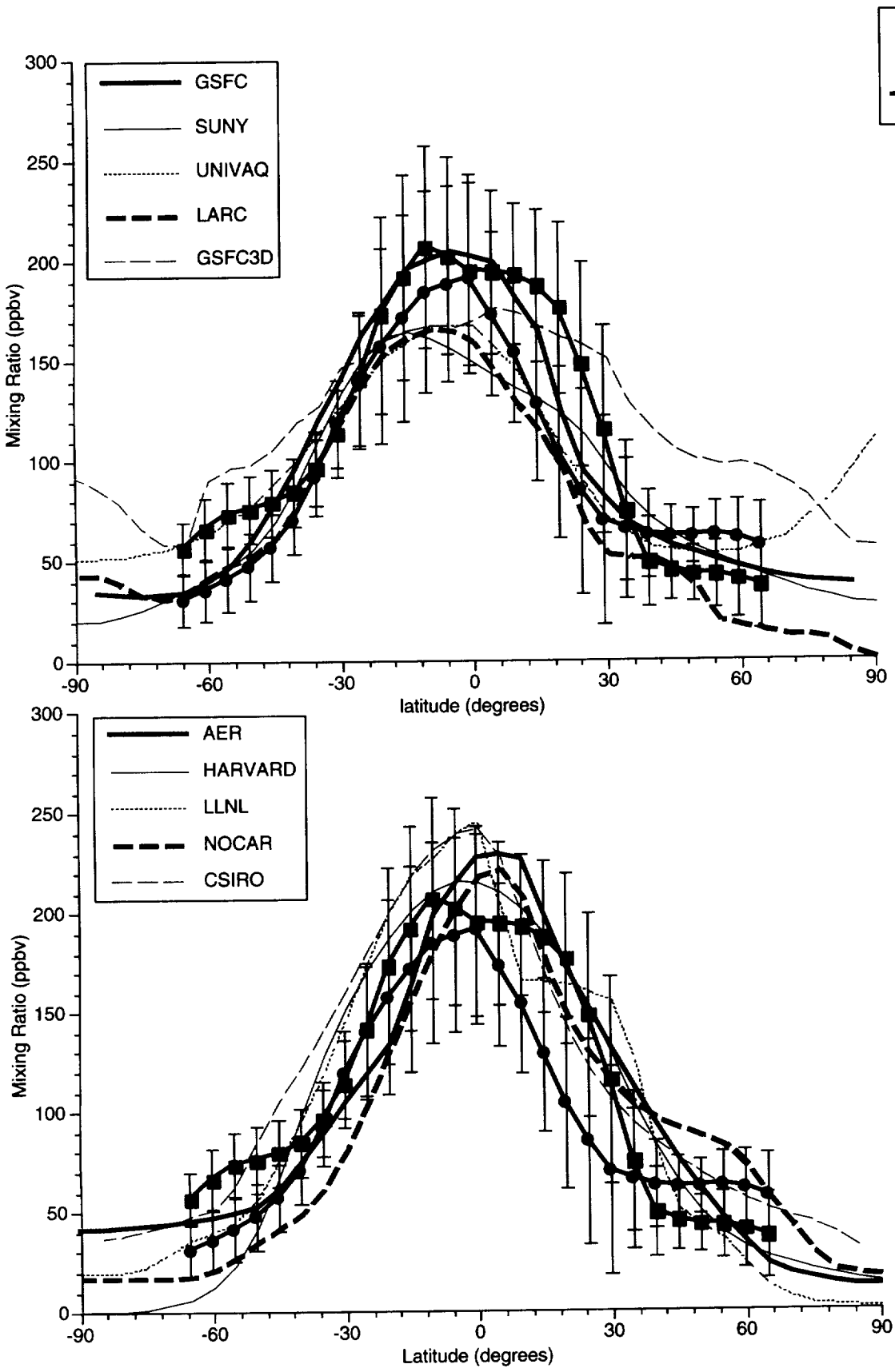

Figure 4: Calculated N2O for spring at 10 mb. Symbols denote the spring 10 mb UARS version 7.0 CLAES data. Error bars represent the meridional variations of the CH4.

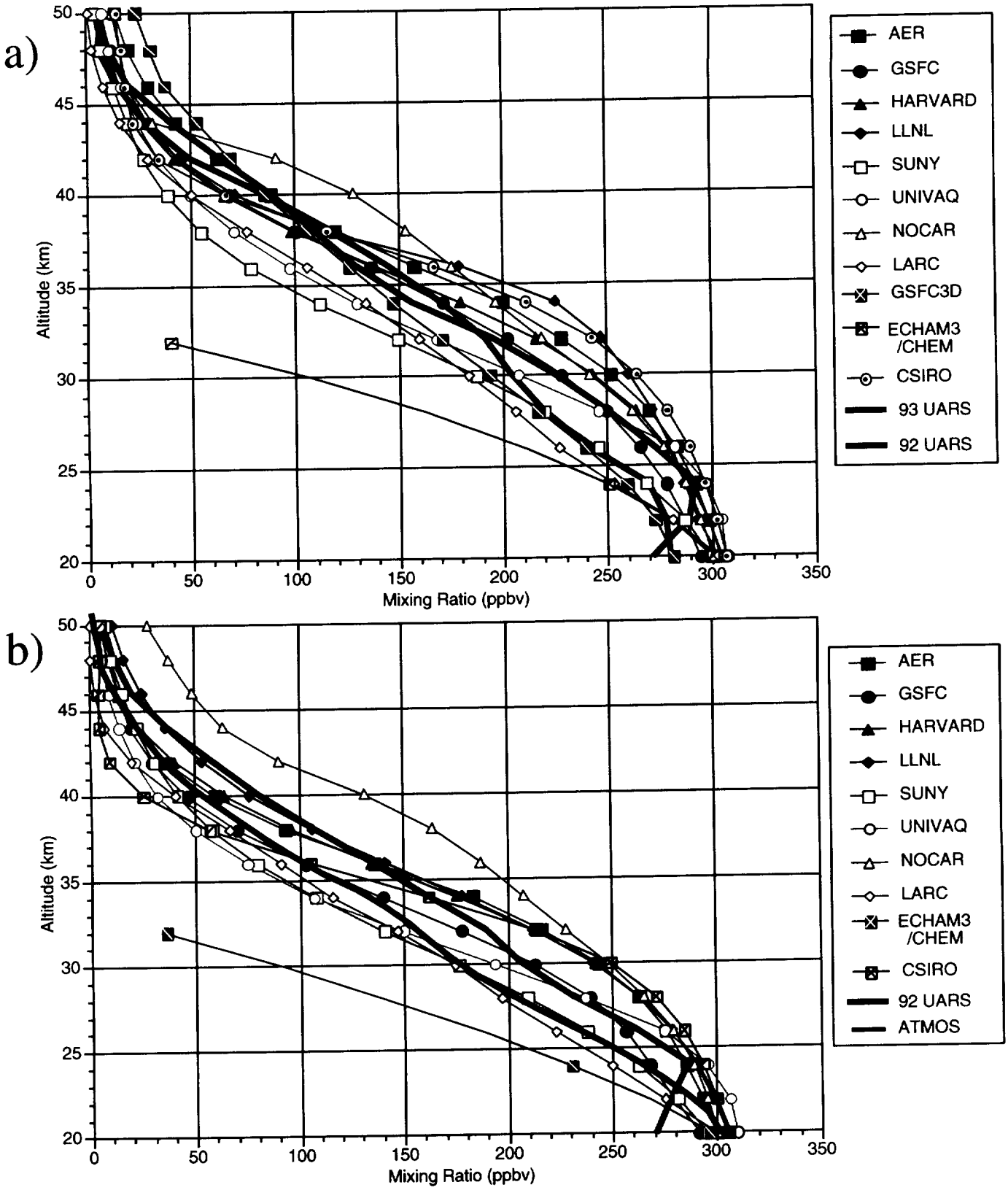

Figure 5: Calculated N2O at the equator between 20 and 50 km. Spring data is in the upper panel (a) while fall values are given in the lower panel (b). Solid lines denote UARS and ATMOS data. The ECHAM3/CHEM calculated points represent the model's resolution. Vallues are shown at 20, 24 and 32 km. The 32 km value represents the top layer of the model, from 0 hPa to 20 hPa and centered at 10 hPa.

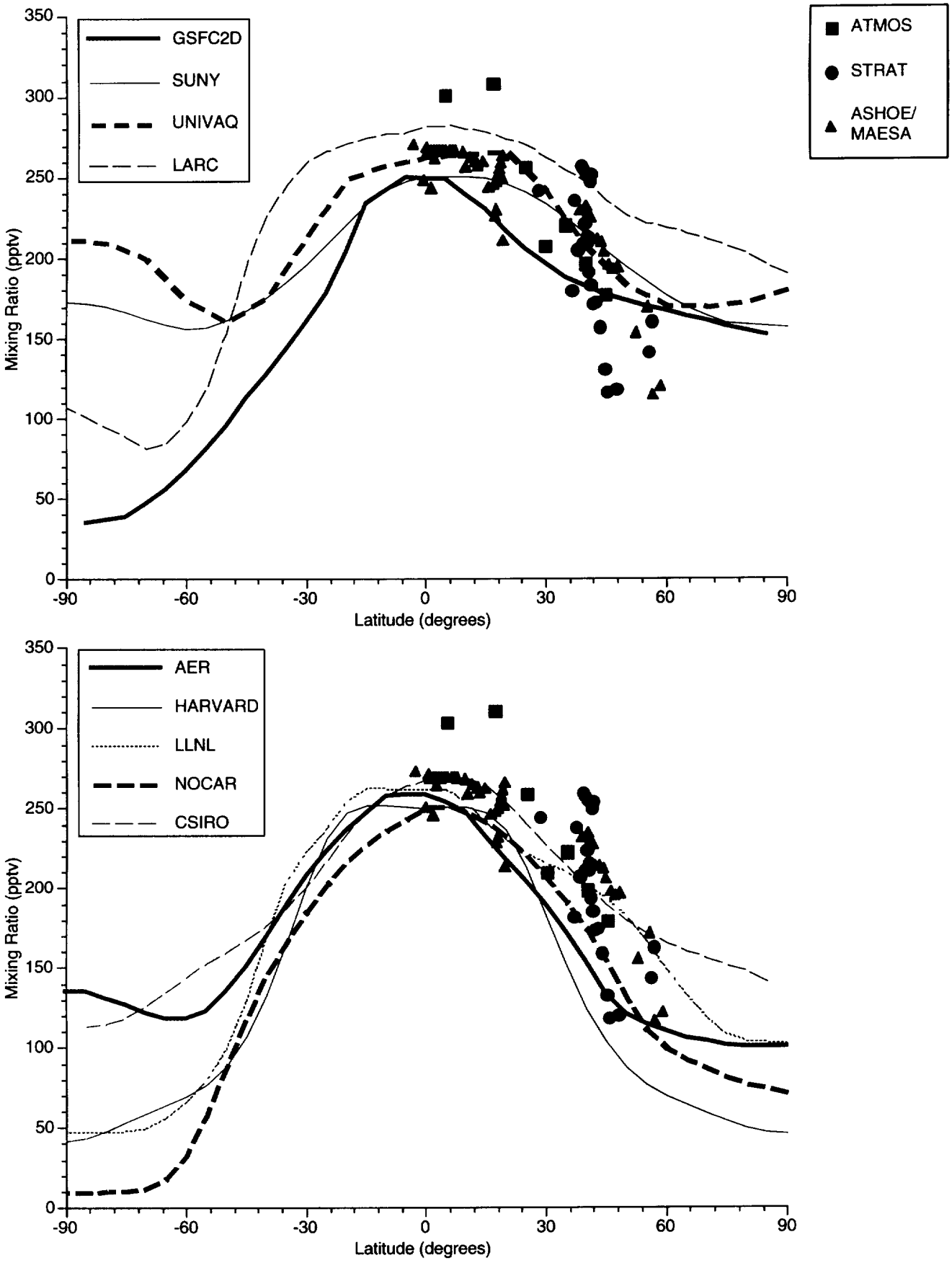

Figure 6: Calculated CFCl3 for fall at 75 mb. Symbols denote the fall ATMOS and flight data from the STRAT and A/M data sets.

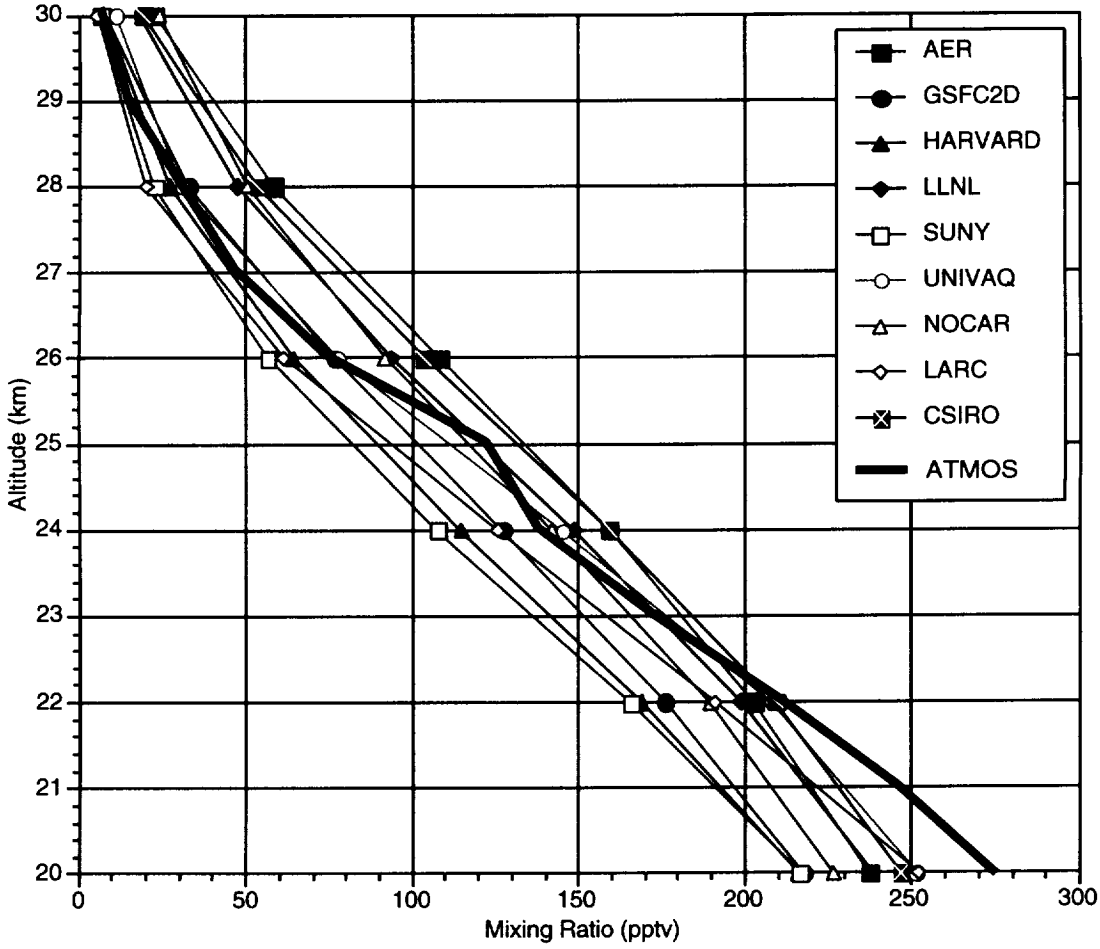

Figure 7: Calculated CFCl3 for fall at the equator between 20 and 30 km. Solid line denotes ATMOS data.

APPENDIX C

"Results of the Model & Measurement Workshop II:
Implications for Future AESA Assessment"

NASA Atmospheric Chemistry Modeling and Data Analysis Program

NAS5-97039: Semi-Annual Report on

Coupling Processes Atmospheric Chemistry and Climate

Results of the Model & Measurement Workshop II: Implications for Future AESA Assessment

Malcolm Ko, AER Inc

Charles Jackman, GSFC

Donald Wuebbles, University of Illinois

With contributions from participants of
The Model and Measurement Workshop II

Outline

- Model and measurement Intercomparison is a way to reduce uncertainties in assessment predictions through model evaluation
- Key conclusions from M&M II
  - what have we accomplished since M&M I?
  - What he new model tests ?
- Where are we relative to the goal of providing reliable estimates of the ozone response to HSCT

Uncertainties in Model Predictions

- Model spread as an indicator of uncertainties
  - Assumption is that all models have equal merits, different results are due to different (valid) approaches
  - This is an acceptable interpretation if there are insufficient observations to test models
- M&M philosophy
  - Identify observations for model testing
  - Compare different approaches to see if certain methods are better than others

Testing components

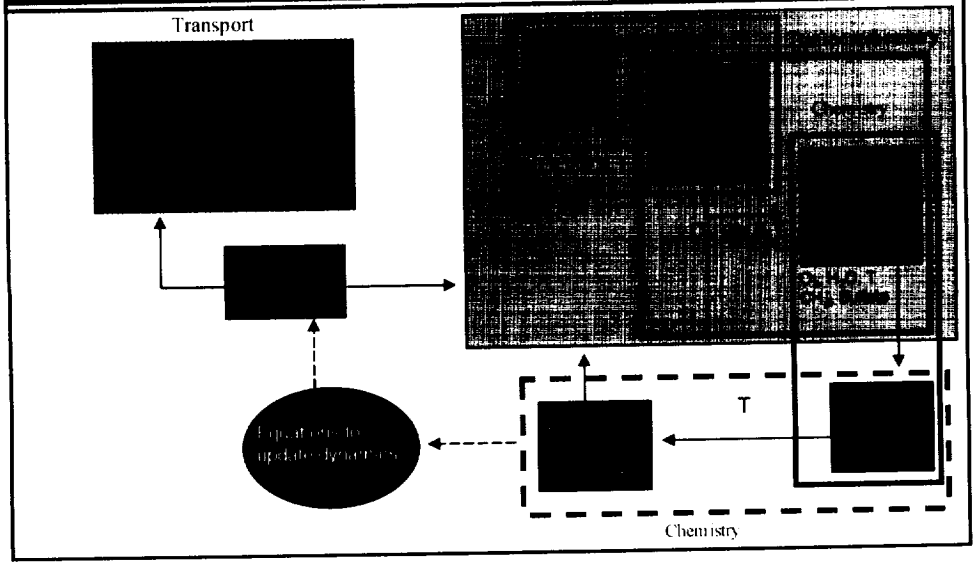

REPORT DOCUMENTATION PAGE

Form Approved
OMB No. 0704-0188

1. AGENCY USE ONLY *(Leave blank)*	2. REPORT DATE	3. REPORT TYPE AND DATES COVERED
	September 1998	Contractor Report

4. TITLE AND SUBTITLE
Semi-Annual Report on Coupling Processes Between Atmospheric Chemistry and Climate

5. FUNDING NUMBERS
NAS5-97039

6. AUTHOR(S)
M.K.W. Ko, D. Weisenstein, R-L Shia, N.D. Sze

7. PERFORMING ORGANIZATION NAME(S) AND ADDRESS (ES)
Atmospheric and Environmental Research, Inc.
840 Memorial Drive
Cambridge, MA 02139-3771

8. PEFORMING ORGANIZATION REPORT NUMBER
P698

9. SPONSORING / MONITORING AGENCY NAME(S) AND ADDRESS (ES)
National Aeronautics and Space Administration
Washington, DC 20546-0001

10. SPONSORING / MONITORING AGENCY REPORT NUMBER
CR—208603

11. SUPPLEMENTARY NOTES
Technical Monitor: R. Stewart, Code 916

12a. DISTRIBUTION / AVAILABILITY STATEMENT
Unclassified–Unlimited
Subject Category: 42
Report available from the NASA Center for AeroSpace Information,
7121 Standard Drive, Hanover, MD 21076-1320. (301) 621-0390.

12b. DISTRIBUTION CODE

13. ABSTRACT *(Maximum 200 words)*

This is the third semi-annual report for NAS5-97039, covering January through June 1998. The overall objective of this project is to improve the understanding of coupling processes between atmospheric chemistry and climate. Model predictions of the future distributions of trace gases in the atmosphere constitute an important component of the input necessary for quantitative assessments of global change. We will concentrate on the changes in ozone and stratospheric sulfate aerosol, with emphasis on how ozone in the lower stratosphere would respond to natural or anthropogenic changes. The key modeling for this work are the AER 2-dimensional chemistry-transport model, the AER 2-dimensional stratosheric sulfate model, and the AER three-wave interactive model with full chemistry. We will continue developing our three-wave model so that we can help NASA determine the strengths and weaknesses of the next generation assessment models.

14. SUBJECT TERMS
Coupling processes, atmospheric chemistry and climate, chemistry-transport model, stratospheric sulfate model, interactive model.

15. NUMBER OF PAGES
56

16. PRICE CODE

17. SECURITY CLASSIFICATION OF REPORT	18. SECURITY CLASSIFICATION OF THIS PAGE	19. SECURITY CLASSIFICATION OF ABSTRACT	20. LIMITATION OF ABSTRACT
Unclassified	Unclassified	Unclassified	UL